Reconnection in strong guide-field turbulent astro-plasmas

J. Büchner[*,], N. Jain & P. Munoz, X. Zhou[**,***]**

Center for Astrophysics and Astronomy, Berlin Institute of Technology (BIT); [*]Max-Planck-Institute for Solar System Research & Georg-August University Göttingen; [**]Max-Planck-Princeton Center for Plasma Physics (MPPC); [***]Purple Mountain Observatory CAS, Nanjing

***


Collaboration: ***D. Groseli and F. Jenko,*** *IPP/MPPC*

Solar eruption (SDO observation)

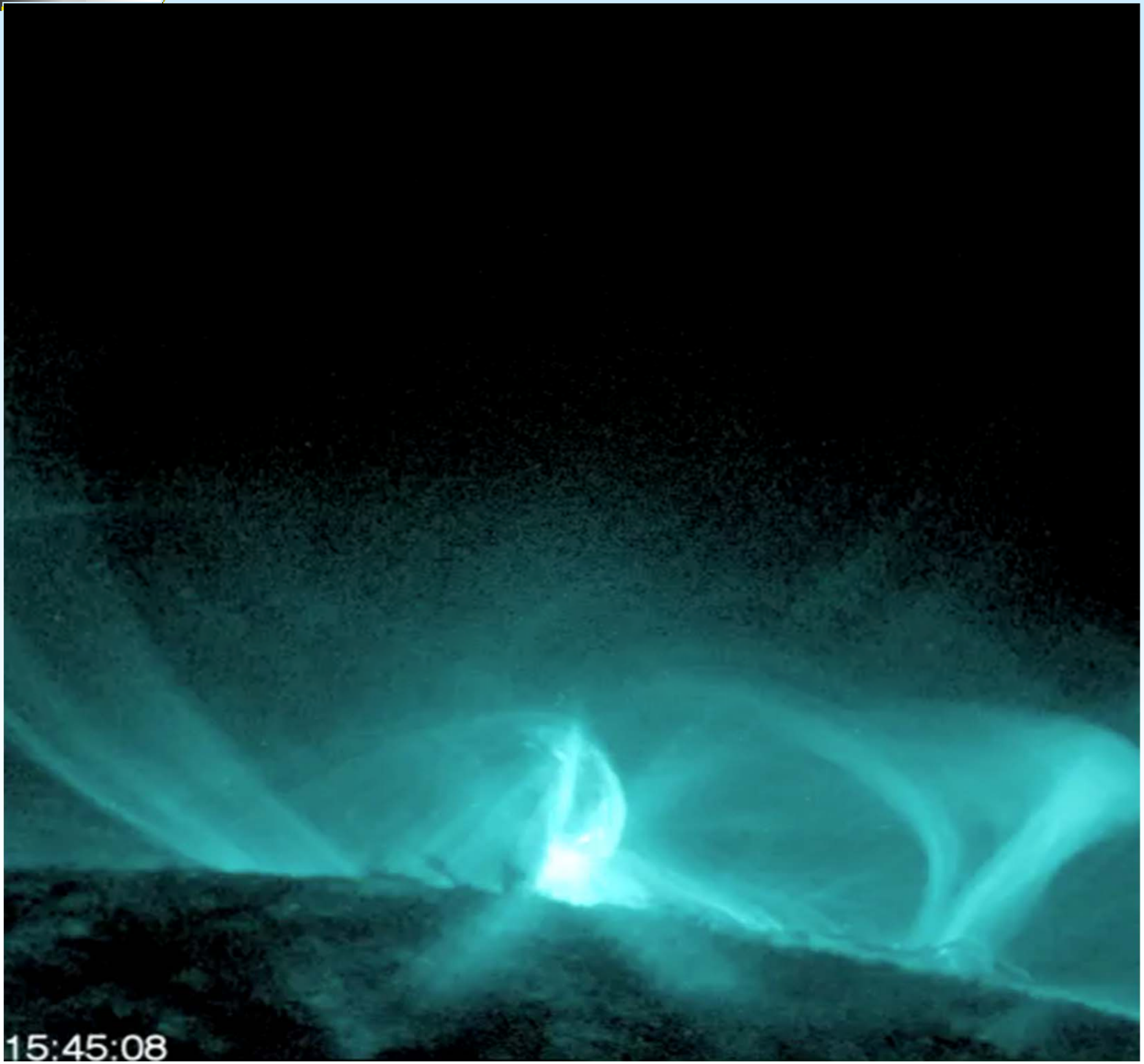

NASA / SDO 131 A, (1.5 MK) on 09/10/2017 X8.2 class flare, fast (> 4,000 km/s) plasma flows detached from the Sun.

These observations do not directly show magnetic fields but their tracers:

supra-thermal electrons, accelerated, perhaps, by magnetic reconnection.

The «standard» flare / CME model

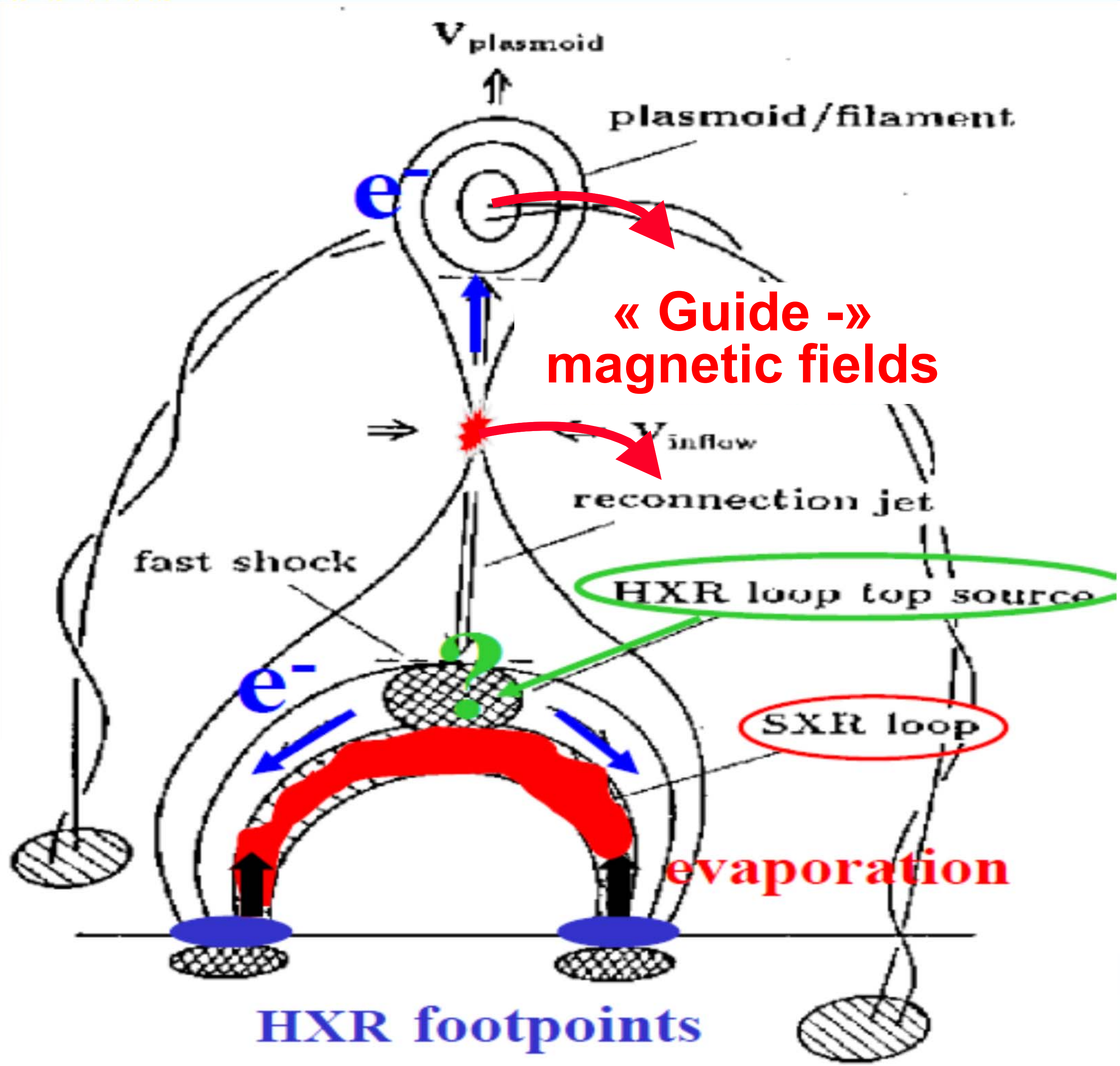

1) Release of magnetic energy by reconnection
2) Particles accelerated & plasma heated (why?)
3) Accelerated electrons produce HXR emission (mostly footpoints)
4) Above loop-top HXR source not understood
5) Collisional losses of accelerated electrons heat chromospheric plasma
6) "Evaporation" fills loop

Reconnection in strong «guide -» magnetic fields – directed out of the reconnection plane

[after: K. Shibata]

Difficulties to release the B-energy

Flare duration
~ Alfven time scale
would explain observations

$$t_{flare} = 10^2 - 10^3 \ s$$

$$t_A = L / V_A = 10 \ s$$

But the magnetic field dissipation time is (for a Spitzer-type resistivity due to electron-ion Coulomb collisions)

$$t_D = L^2 / \eta_D \approx 10^{14} \left(\frac{L}{10^9 cm} \right)^2 \left(\frac{T}{10^6 K} \right)^{3/2} \quad s$$

$$\eta_D = \eta_{D,Spitzer} \approx 10^4 \left(\frac{T}{10^6 K} \right)^{-3/2} \quad cm^2 / s$$

Hence: Joule dissipation is much too inefficient, indicator: R_m

$$R_m = t_D / t_A >> 1$$

"(Magneto-hydromagnetics is a fascinating subject and one which is very imperfectly understood; but it is also one in which the probability of being led astray by seductive theories is very high" (Cowling 1953)

Reconnection at large S & λ = L / ϱ

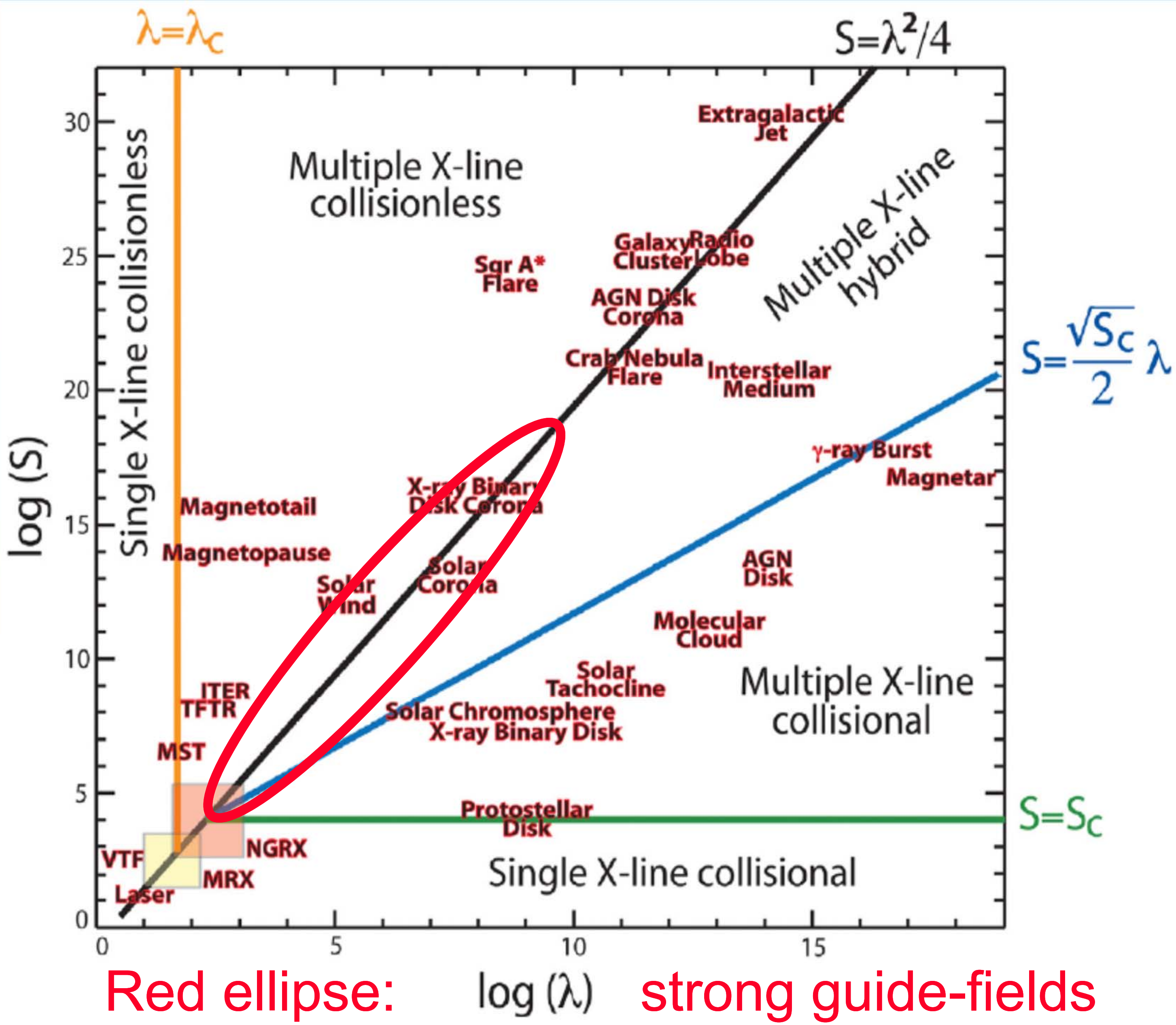

Red ellipse: strong guide-fields

S = Lundquist number, i.e. the Reynolds number for a Alfven speed flows:

$$S \equiv \frac{\mu_0 L_{CS} V_A}{\eta}$$

λ = L (system size) / ϱ (ion Larmor radius)

[Ji & Daughton, 2011]

Huge *S* -> these plasmas are turbulent!

Turbulence enhanced reconnection?

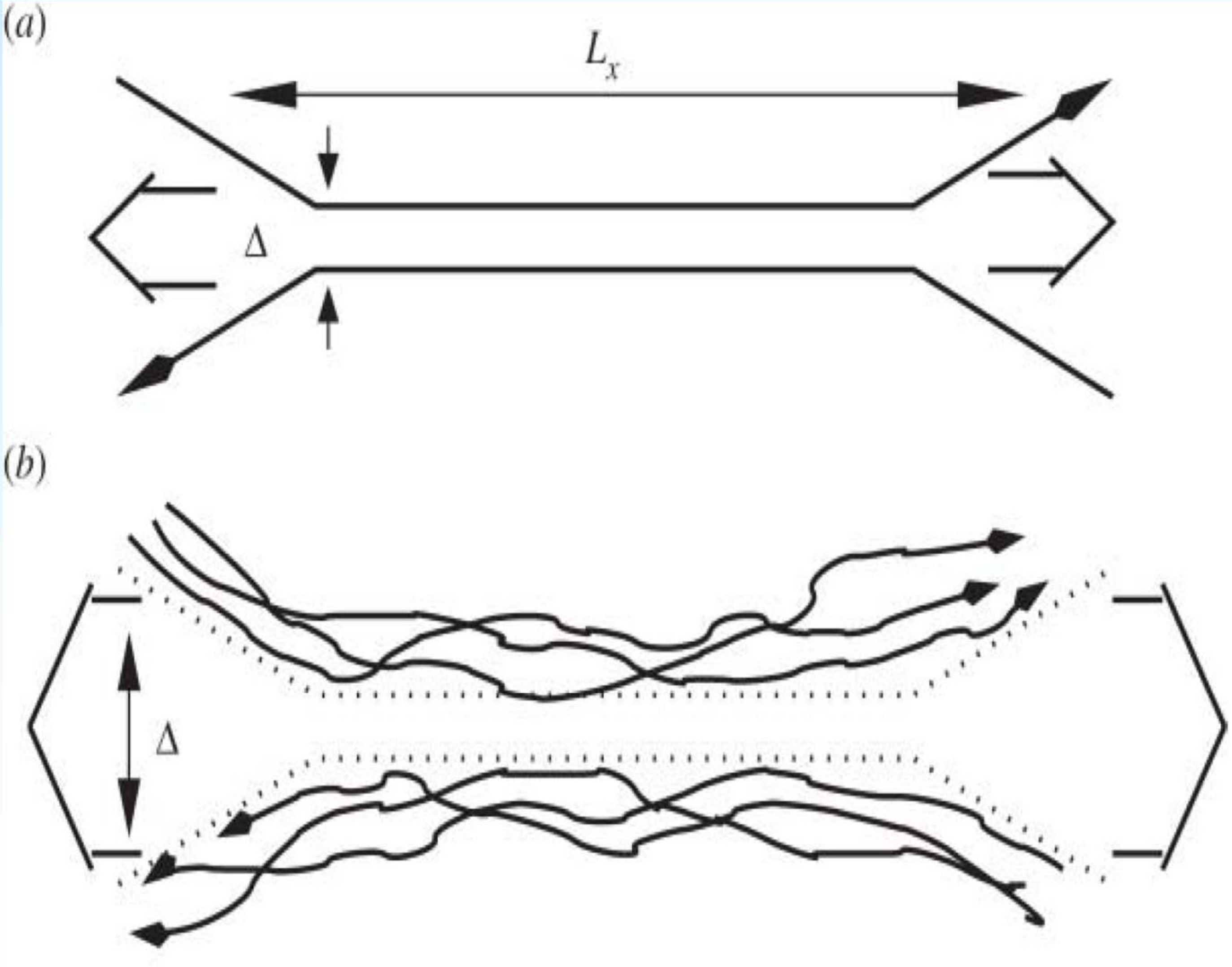

[Matthews & Lamkin, 1985; Lazarian & Visnjak, 1999] conjectured: „… the narrow outflow channels of laminar reconnection (a) could effectively be widened by turbulence (b)“

Observed turbulence

ESA-CLUSTER multi-spacecraft observed Alfvenic turbulence with a steeper spectrum beyond the proton scales (blue line).

Intermittency found at scales λ_i - ρ_i (close to dissipation range !) indicate the formation of small-scale coherent structures - magnetic islands, current sheets?

Dissipation in coherent structures with d~ λ_i - ρ_i larger than wave damping around Ω_{ci} -> Conjecture: small scale reconnection may be the dominant mechanism for energy dissipation at ion scales.

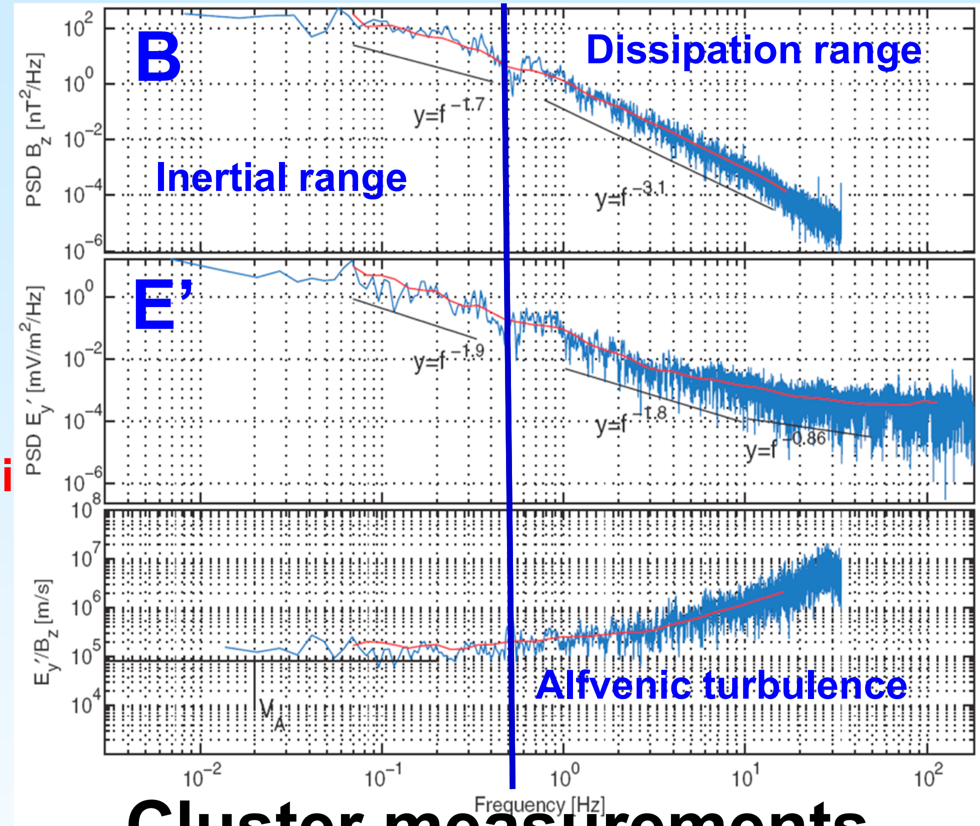

Cluster measurements

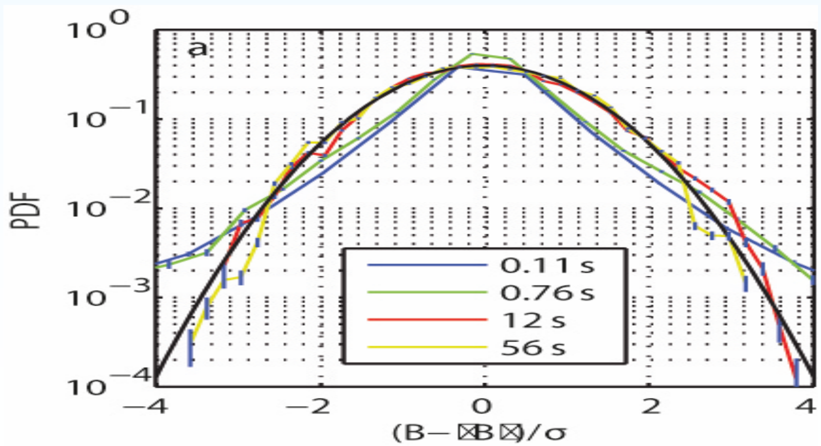

A.I.K.E.F. hybrid code simulations

- 2-D hybrid simulations by a 3-D parallel A.I.K.E.F. code [Mueller et al, 2011]
  - Ions as particles and electrons as inertialless fluid
- Initial conditions:
  - A uniform plasma (similar to Franci et al., 2015)
- – random phased equal amplitude Alfvenic fluctuations in the range

  $k_{min}\, d_i < k\, d_i < 0.2 < k_{break}\, d_i \approx 1$

  - An external magnetic field perpendicular to the 2-D simulation plane. (B_{guide}~1)
- Periodic boundaries.
- Simulation parameters:
  - box size: 256 $d_i \times$ 256 d_i
  - Grid points: up to 2048 $\times$ 2048
  - Particles per cell: 500

Result: current sheets created / strong antiparallel magnetic field compnents (B_{rec} ~ B_g)

Current sheet diagnostics: $J_{||}$

Hybrid code simulations of Alfvenic turbulence for moderate R_m that turbulence spontaneously formed current sheets at kinetic scales which decay by kinetic scale reconnection. Here: $J_z=J_{||}$ [from Jain & Büchner, 2019]

Ion heating near current sheets

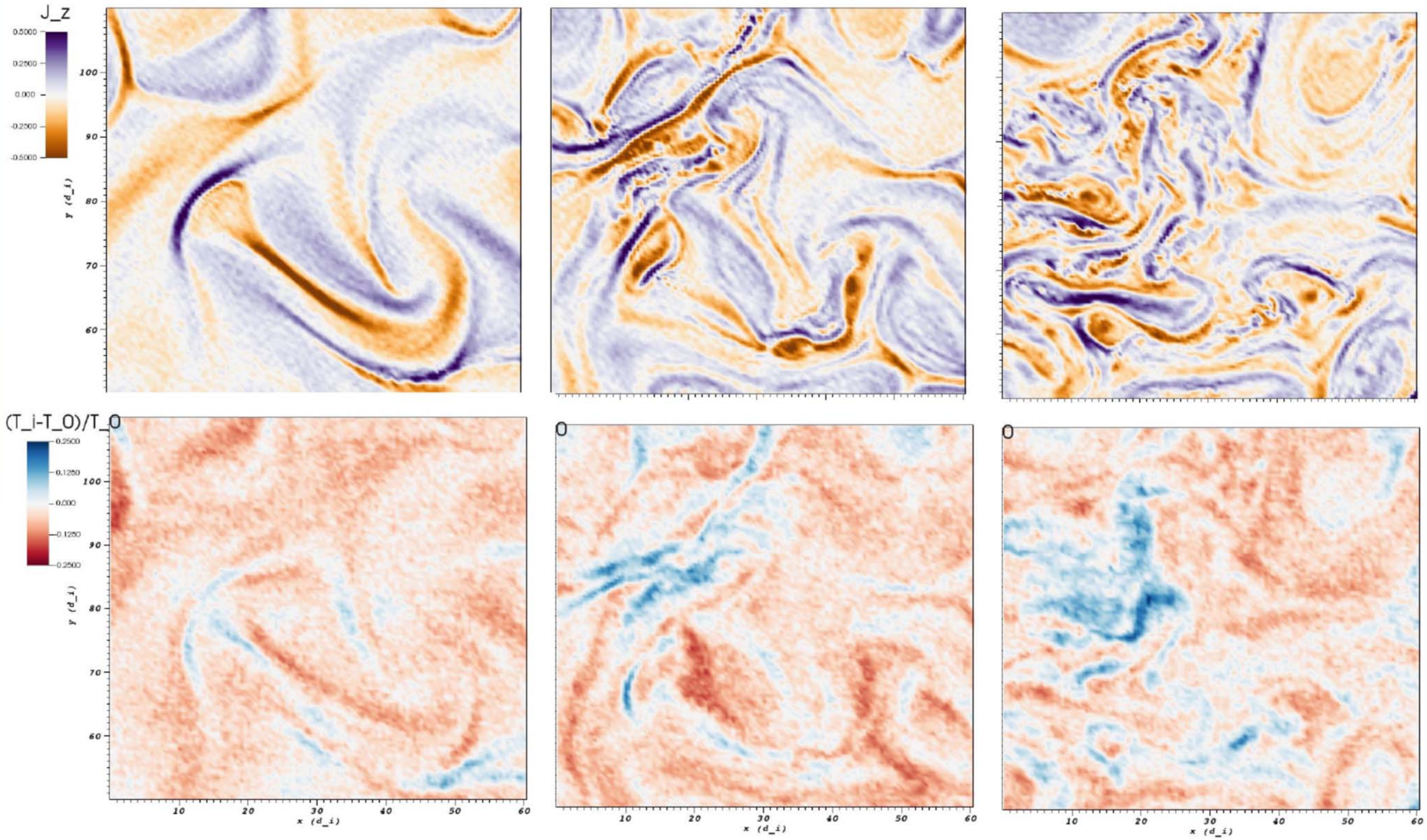

Blue => parallel red => anti-parallel

Blue => enhanced red => reduced temp.

$t\,\Omega_{ci} = 50$ $t\,\Omega_{ci} = 100$ $t\,\Omega_{ci} = 150$

from: [Jain, Büchner, 2019]

Spectral breaks

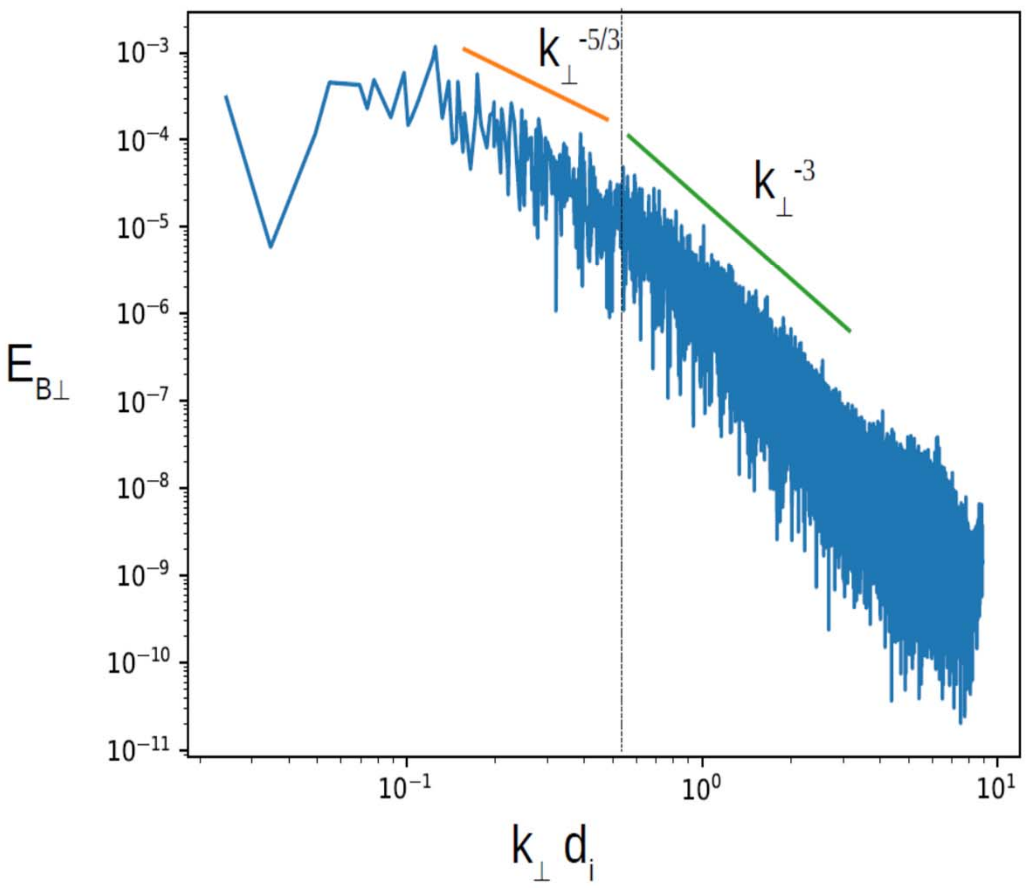

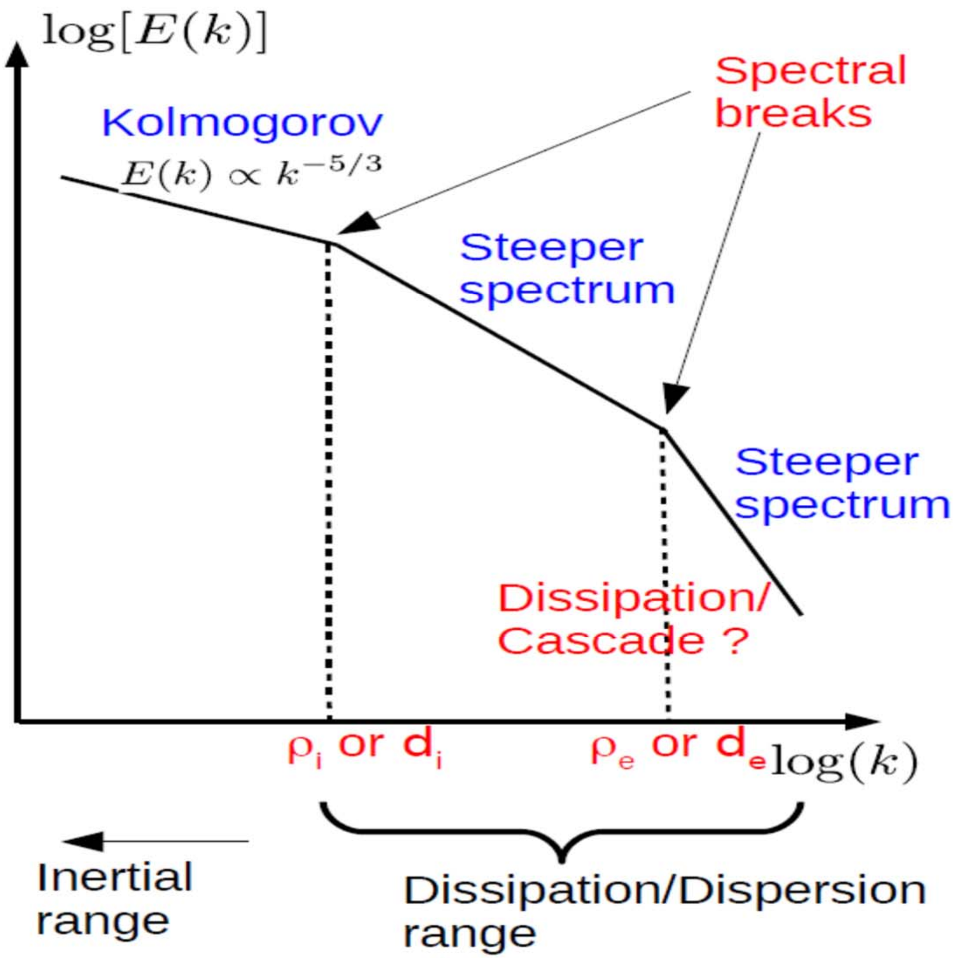

Hybrid code results, but what about dissipation scales?

Gyrokinetic simulations

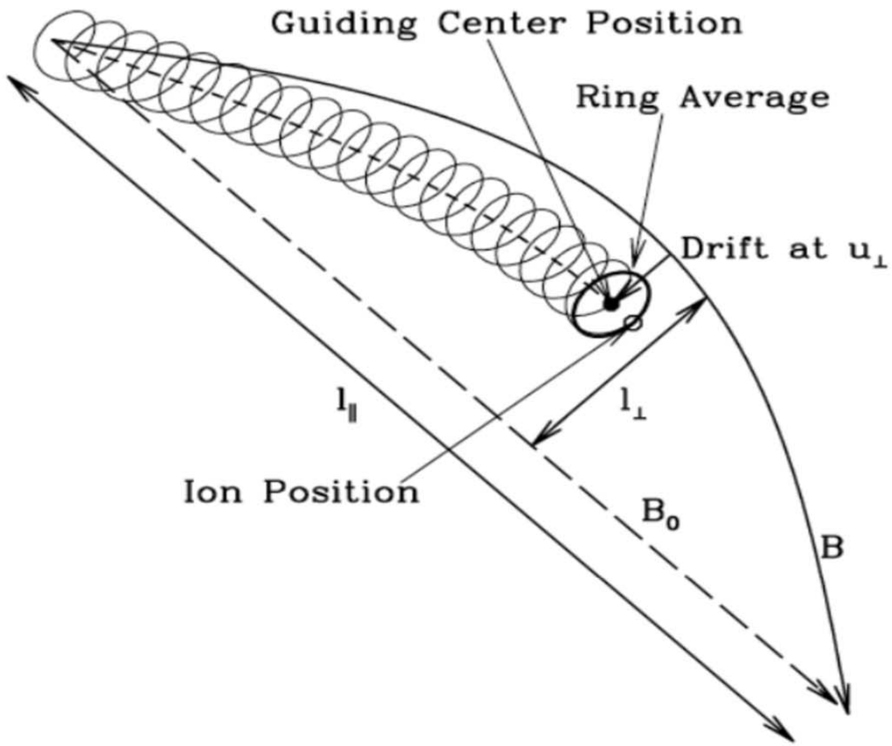

Strong background magnetic field:
Eliminate fast gyromotion; consider (only) dynamics of **guiding centers**

$$f = f(\mathbf{X}, v_{||}, \mu; t)$$

$$\frac{\partial f}{\partial t} + \dot{\mathbf{X}} \cdot \frac{\partial f}{\partial \mathbf{X}} + \dot{v}_{||} \frac{\partial f}{\partial v_{||}} = 0$$

$$\dot{\mathbf{X}} = v_{||}\,\mathbf{b} + \frac{B}{B_{||}^*}\left(\frac{v_{||}}{B}\bar{\mathbf{B}}_{1\perp} + \frac{c}{B^2}\bar{\mathbf{E}}_1 \times \mathbf{B} + \frac{\mu}{m\Omega}\mathbf{b} \times \nabla(B + \bar{B}_{1||}) + \frac{v_{||}^2}{\Omega}(\nabla \times \mathbf{b})_\perp\right)$$

$$\dot{v}_{||} = \frac{\dot{\mathbf{X}}}{m v_{||}} \cdot \left(e\bar{\mathbf{E}}_1 - \mu\nabla(B + \bar{B}_{1||})\right) \qquad \dot{\mu} = 0$$

magnetic moment (adiabatic invariant)

Creation of CSs in turbulence (2D)

Random initial (t=0) $f_1 \sim k_x^{-1}\, k_y^{-1}$ + small v-space perturbations

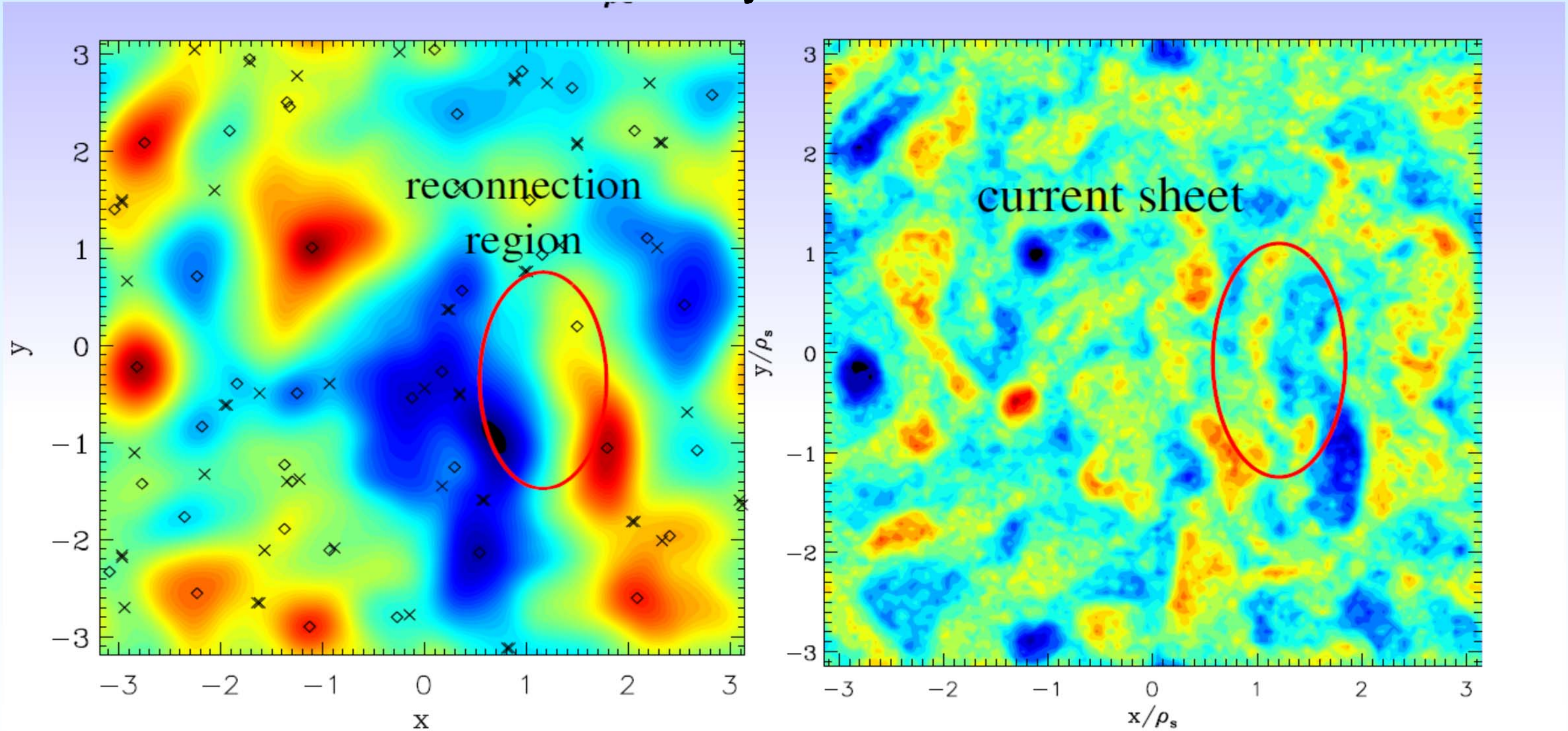

$A_{||}$ -> islands diagnosed (left) and between them current sheets diagnosed in $j_{||}$ (right); scales $\lambda \sim d_e = c/\omega_{pe}$ [from Told et al., 2013]

3D PIC code simulations (OSIRIS)

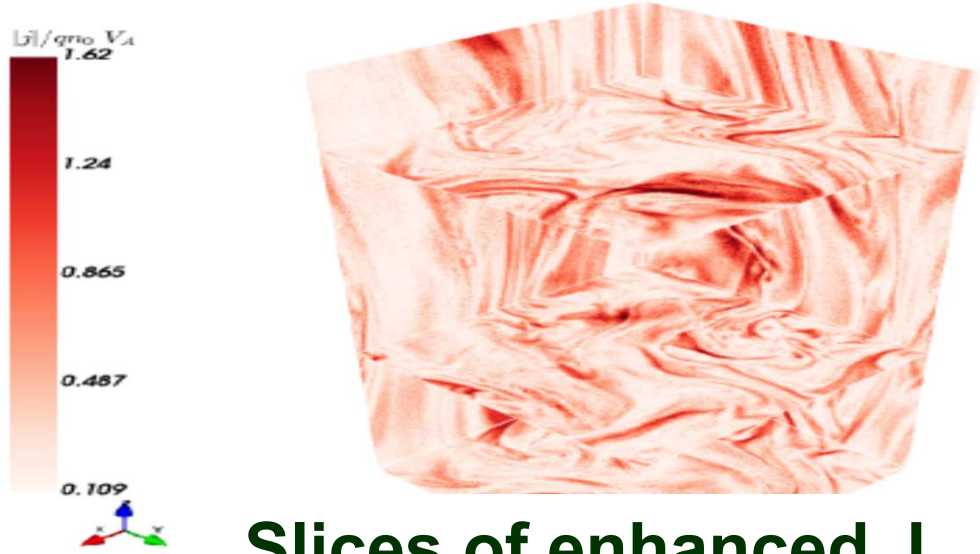

Slices of enhanced J_z

3D kinetic evolution of a collisionless turbulent plasma, Tang-Orzang vortex initialization, OSIRIS PIC code simulation results [Groselij et al., 2018]

Resources used per simulation	3D	
# CPU cores	32768	
Memory [TB]	11	
Total (aggregate) runtime [days]	5	
Amount of data generated [TB]	0.7	

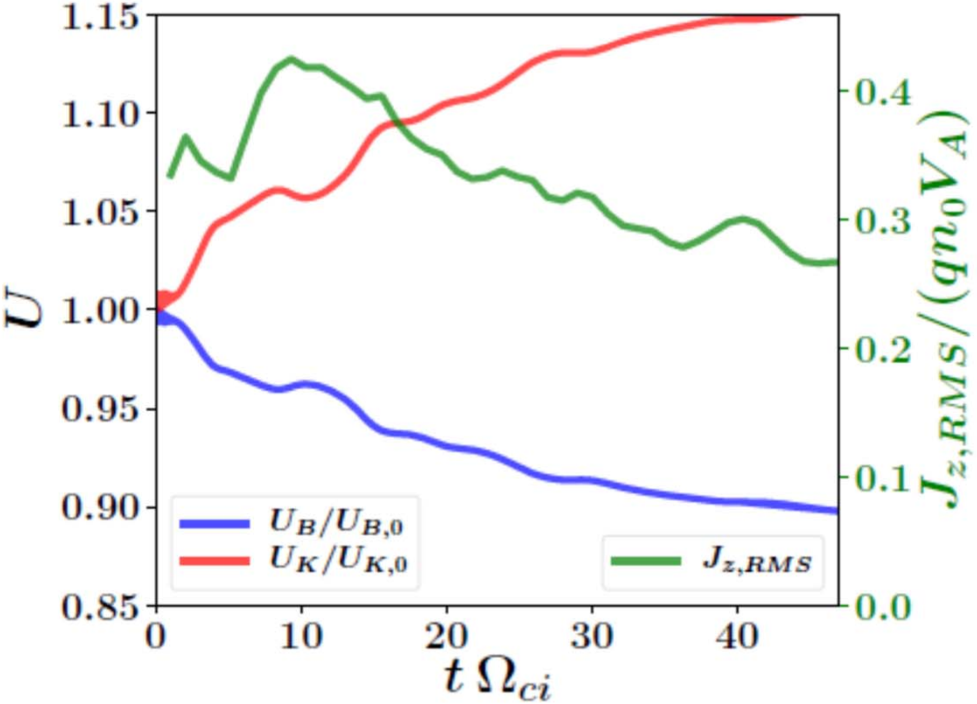

Green: current density (rms) – first increases, then decreases

Blue: magnetic field energy decreases all the way

Red: Kinetic energy increases all the way

3D PIC simulations (ACRONYM)

Force free current sheets

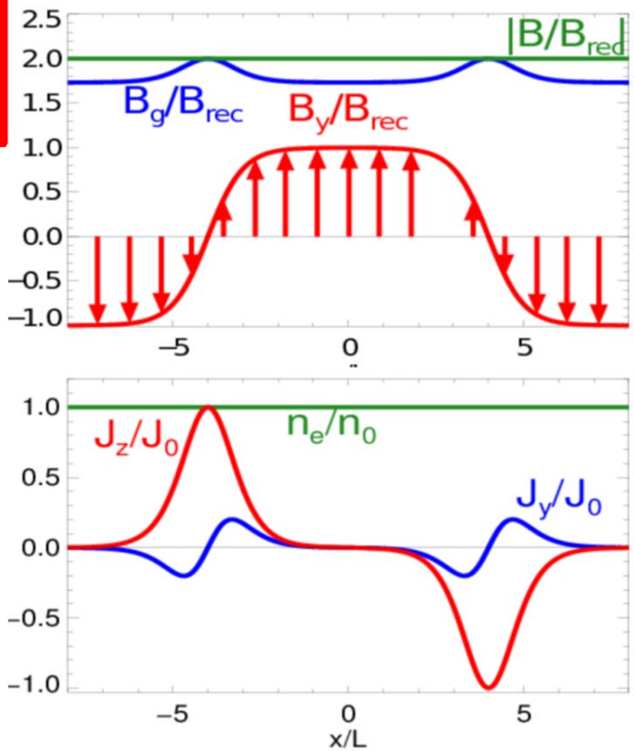

Physical parameters

$$b_g = B_z/B_{\infty y} = 0 \ldots 8$$

$$L/d_i = 0.5, M_i/m_e = 100$$

$$\omega_{pe}/\Omega_{ce} = 4.16, T_i/T_e = 1.0$$

$$n_b/n_0 = 0.2, d_{i/e} = c/\omega_{pi/pe}$$

Initial condition - perturbation:

$$\delta A_z = \delta P B_{\infty y} \frac{L_y}{2\pi} \sin\left(\frac{2\pi\,(y + L_y/4)}{L_y}\right) \sin^2\left(\frac{2\pi x}{L_x}\right)$$

Numerical parameters:

200 ppc (e+i) everywhere

L_x x L_y x L_z = $(4x8x16)d_i^3$

512x512x1024 (10^8) grid points

2 x 10^10 particles

$$\rho_{e,bg} = v_{th,e}/(b_g \Omega_{ce})$$

$$\Delta x/\rho_{e,bg} = 0.166 b_g$$

$$\Delta t = (1/23.9)\omega_{pe}^{-1}$$

$$CFL : c\Delta t/\Delta x = 0.5.$$

Kinetic reconnection causes small (electron-) scale turbulence

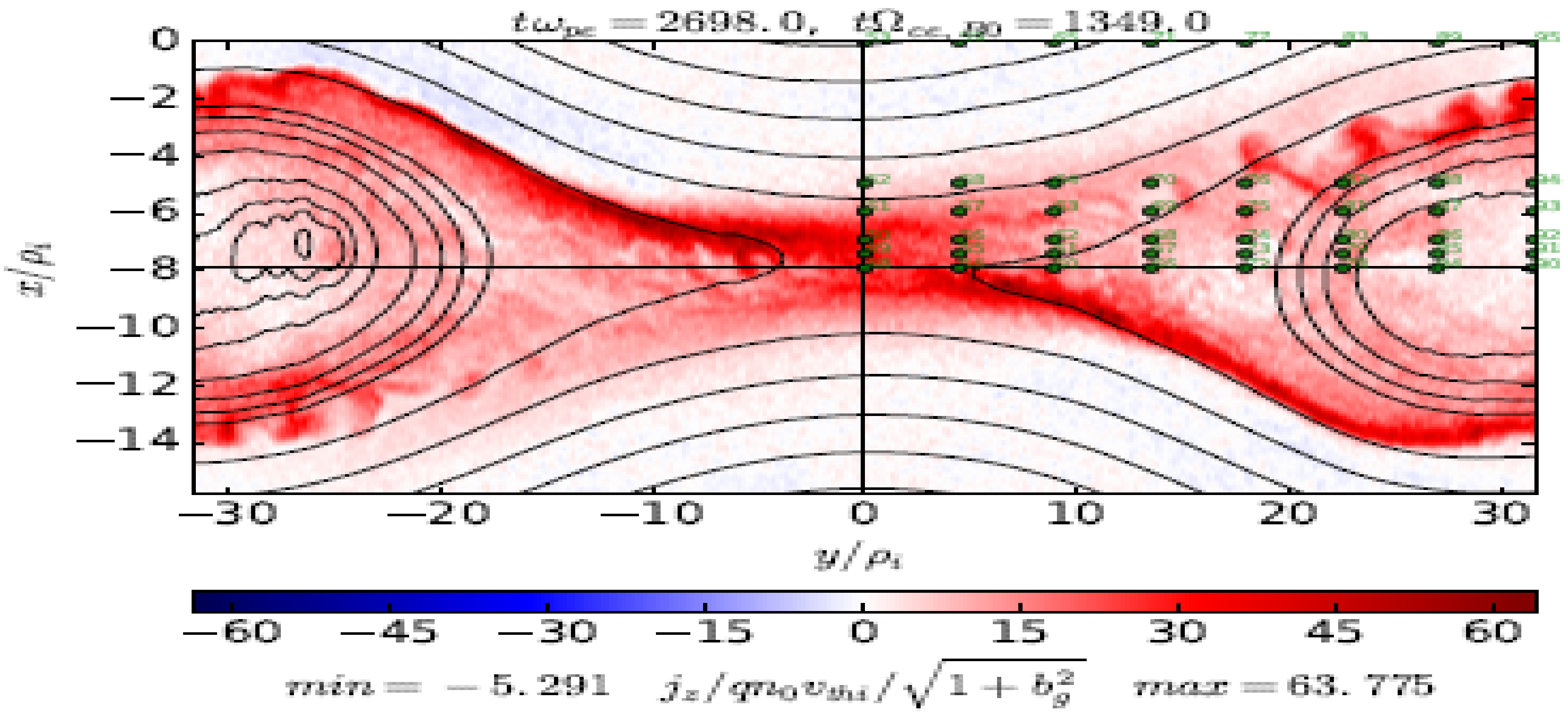

Here: out-of plane current density (j_z) at t Ω_{ci} = 13.5.

Green dots: local diagnostics [from Munoz & JB, 2018a]

δB^2 – dynamic turbulence spectra

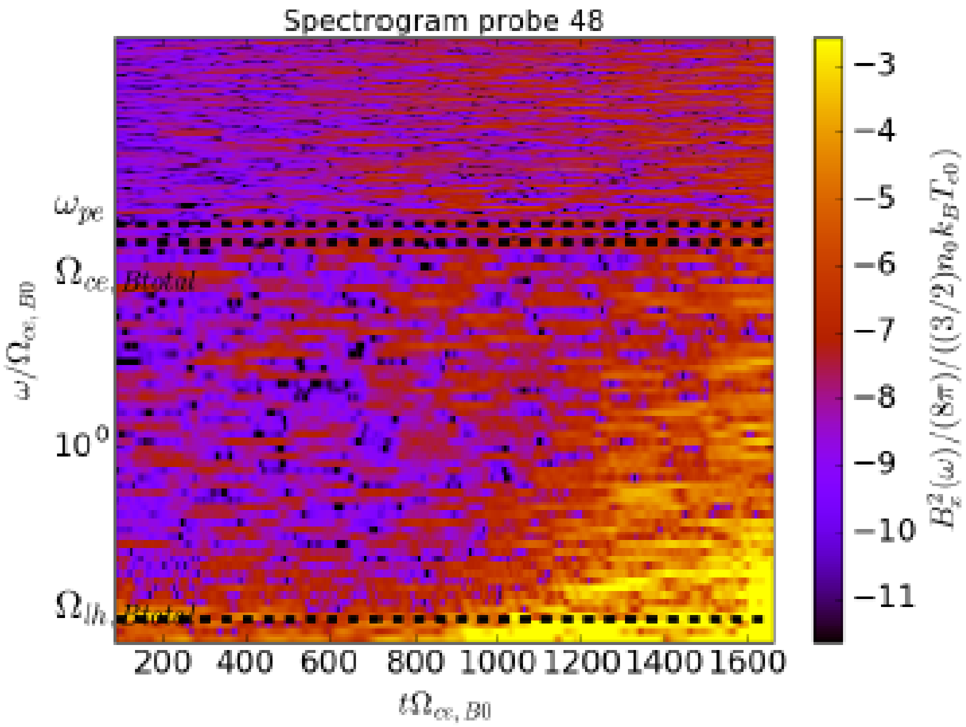

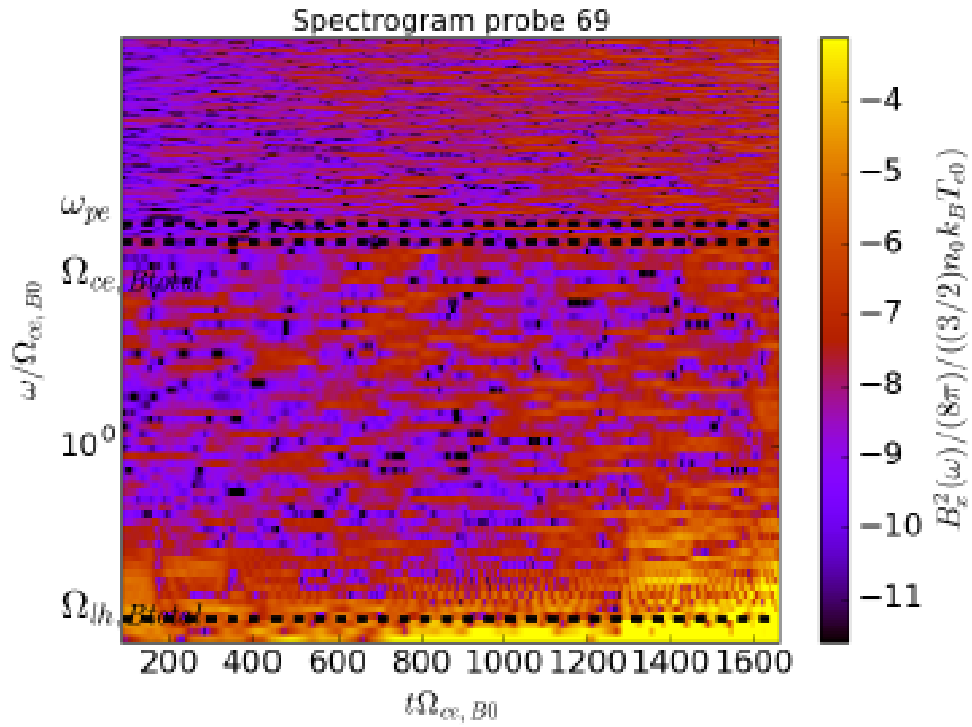

Center of reconnection **Separatrix region**

After $t\,\Omega_{ci} = 9$ ($t\,\Omega_{ce} \sim 900$) the spectrum of the turbulence begins to extend up to the electron plasma frequencies !

[from Munoz & JB, 2018a]

Current energy causes turbulence

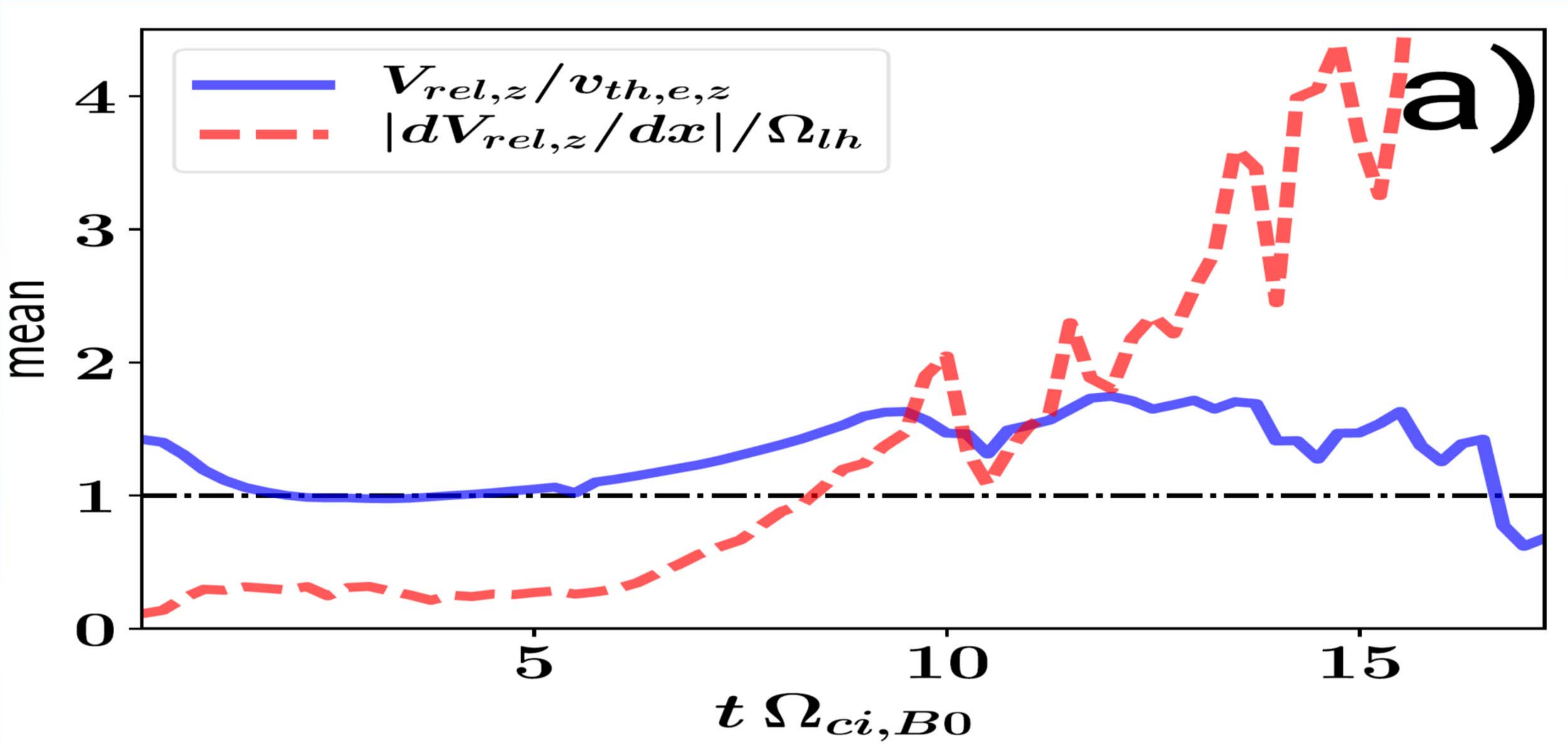

Mean values along the reconnection X-line (averaged along z-direction): streaming - Vrel,z (solid line) & shear flow - |dVrel,z/dx| (red dashed line) Dash-dotted line:Bunemann instability threshold.

Reconnection becomes very fast

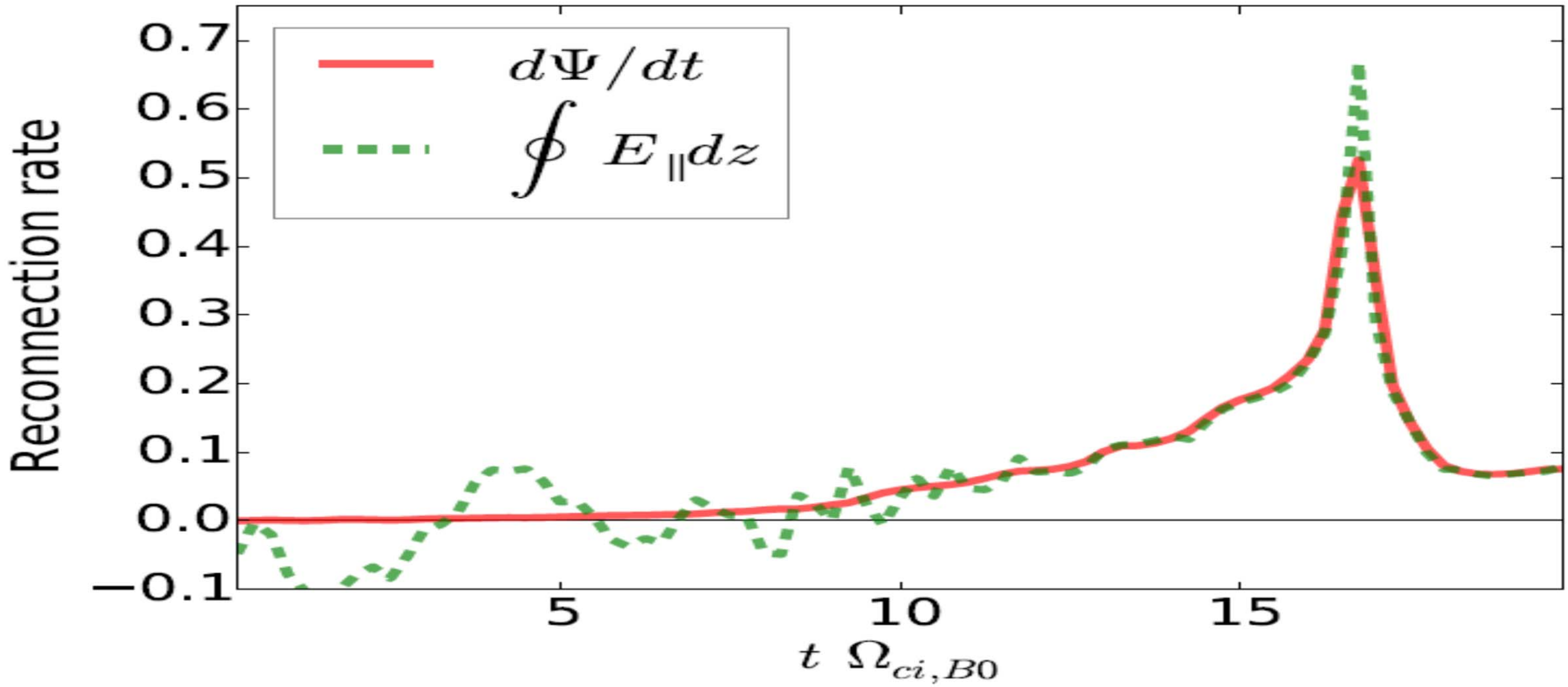

Red/green: reconnection rate determined by two methods. The reconnection rate is strongly enhanced during the non-linear evolution of reconnection – net-$E_{\parallel}$. Saturation at t Ω_{ci}=16, after the B-flux is exhausted.

Turbulence <-> reconnection rate

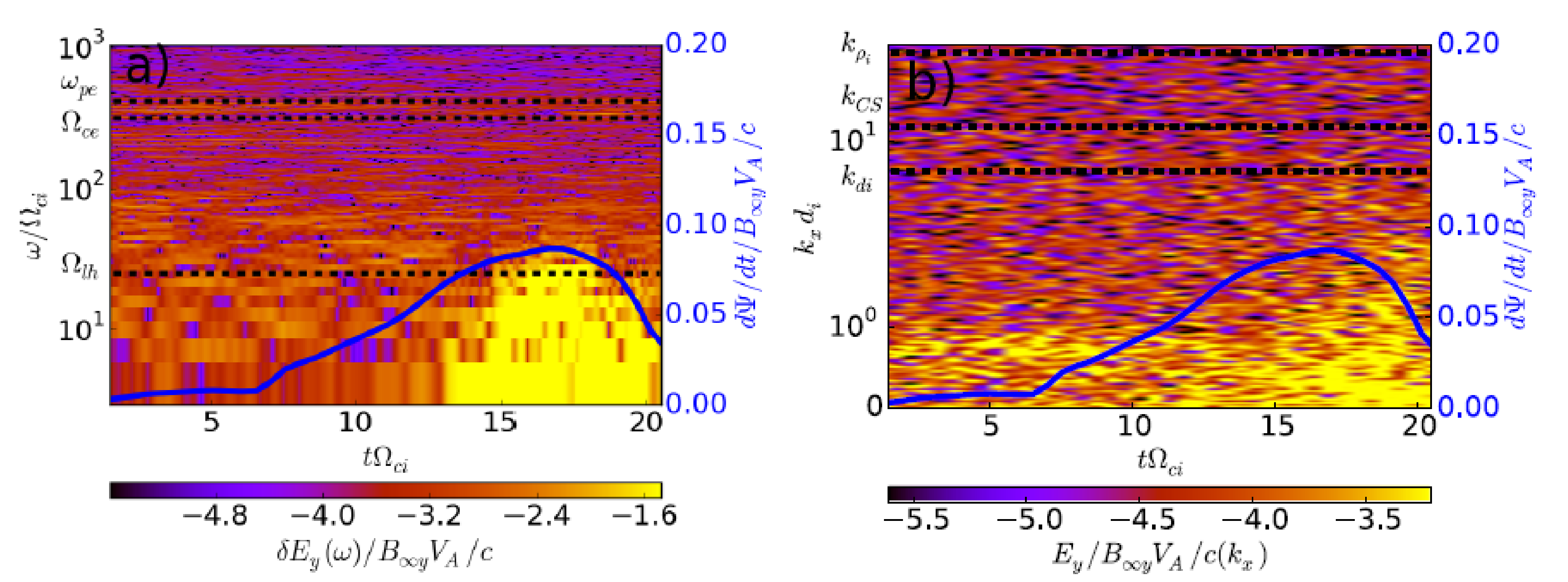

Evolution of the frequency spectrum: indicate obliquely propagating broadband waves / turbulence

Evolution of the wave-number (kx) spectrum: broadband in 0.3< k d_i < 4; k_x~$k_{||}$; U~6-8 Vthi -> electron beam resonance ?!

The reconnection rate is shown by a solid blue line.

Secondary structure formation

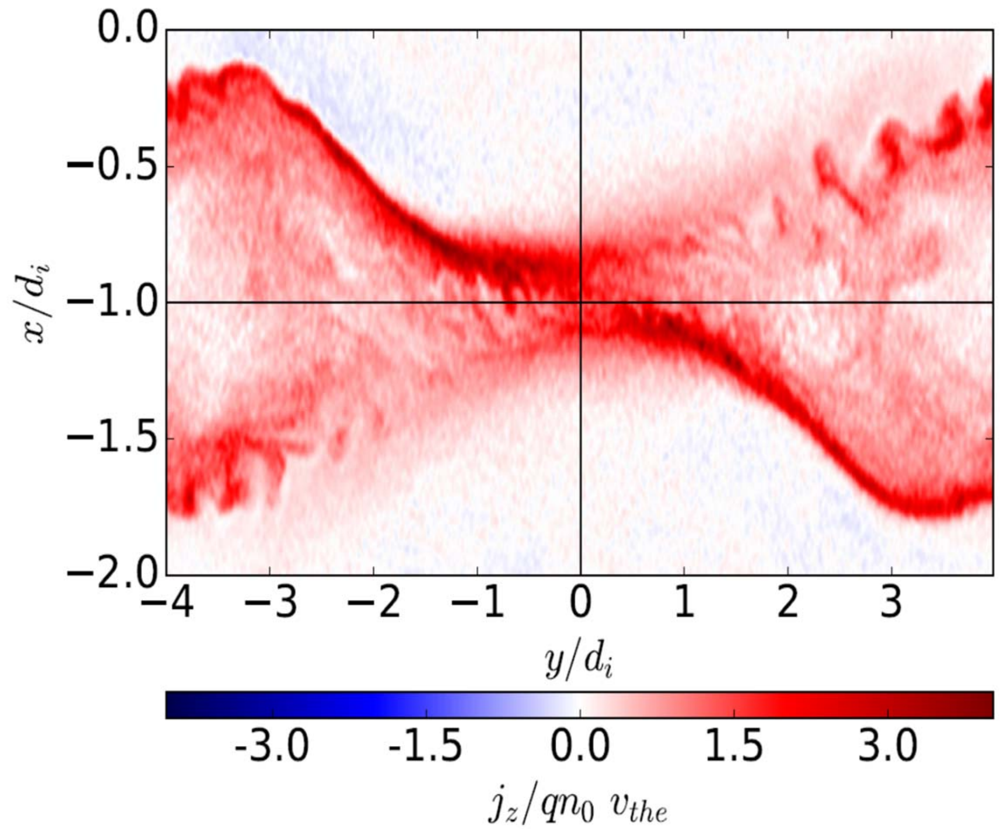

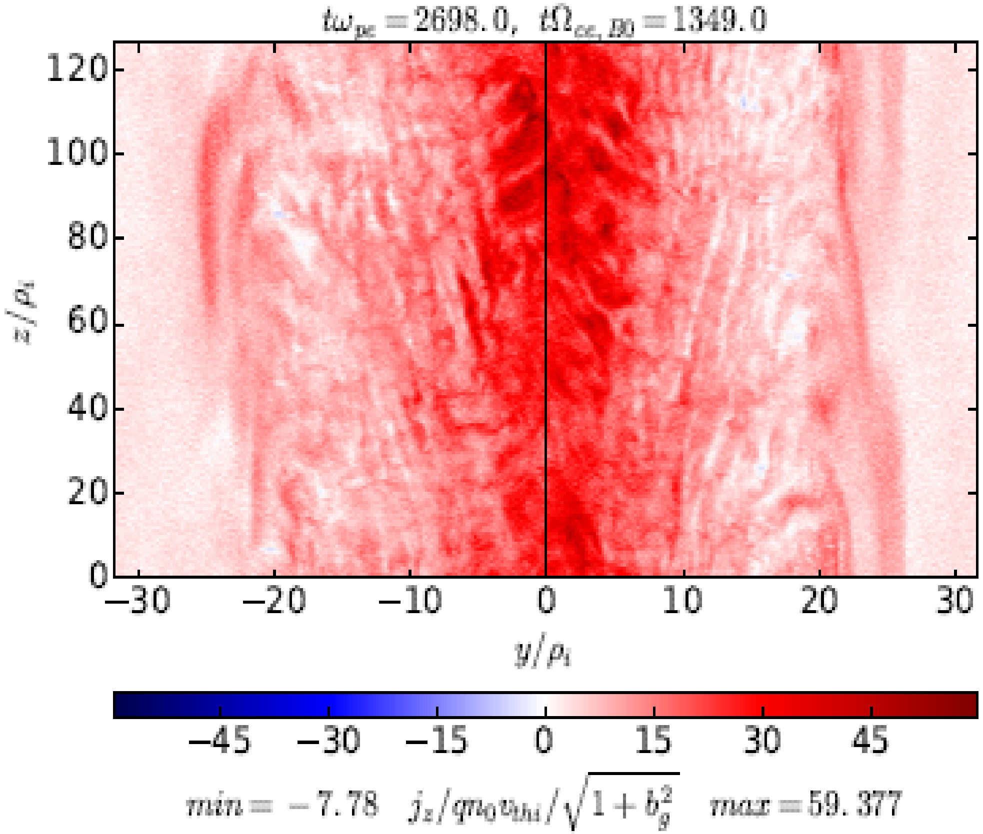

Reconnection plane (perp) <-> Plane along the X-line

Filamentation along X-line at t Ω_{ci} =13.5 - reconnection and turbulence are fully developed [Munoz & JB, 2018b]

Parallel electric field structures

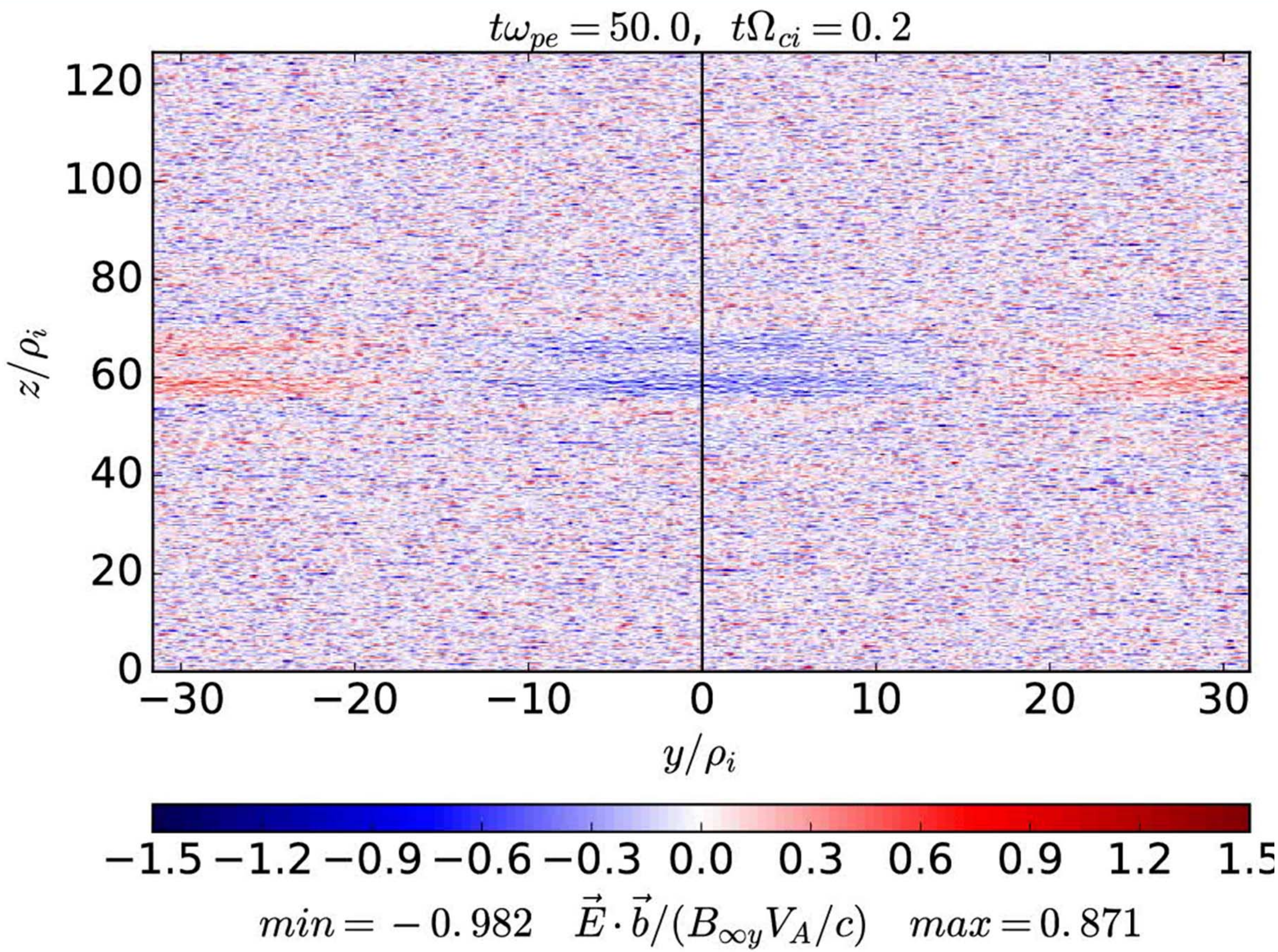

Here shown:

Parallel (i.e. magnetic-field-aligned) components of the fluctuating electric field:

Out of the turbulence structures grow

from [Munoz & Büchner, 2018b]

Electron energization

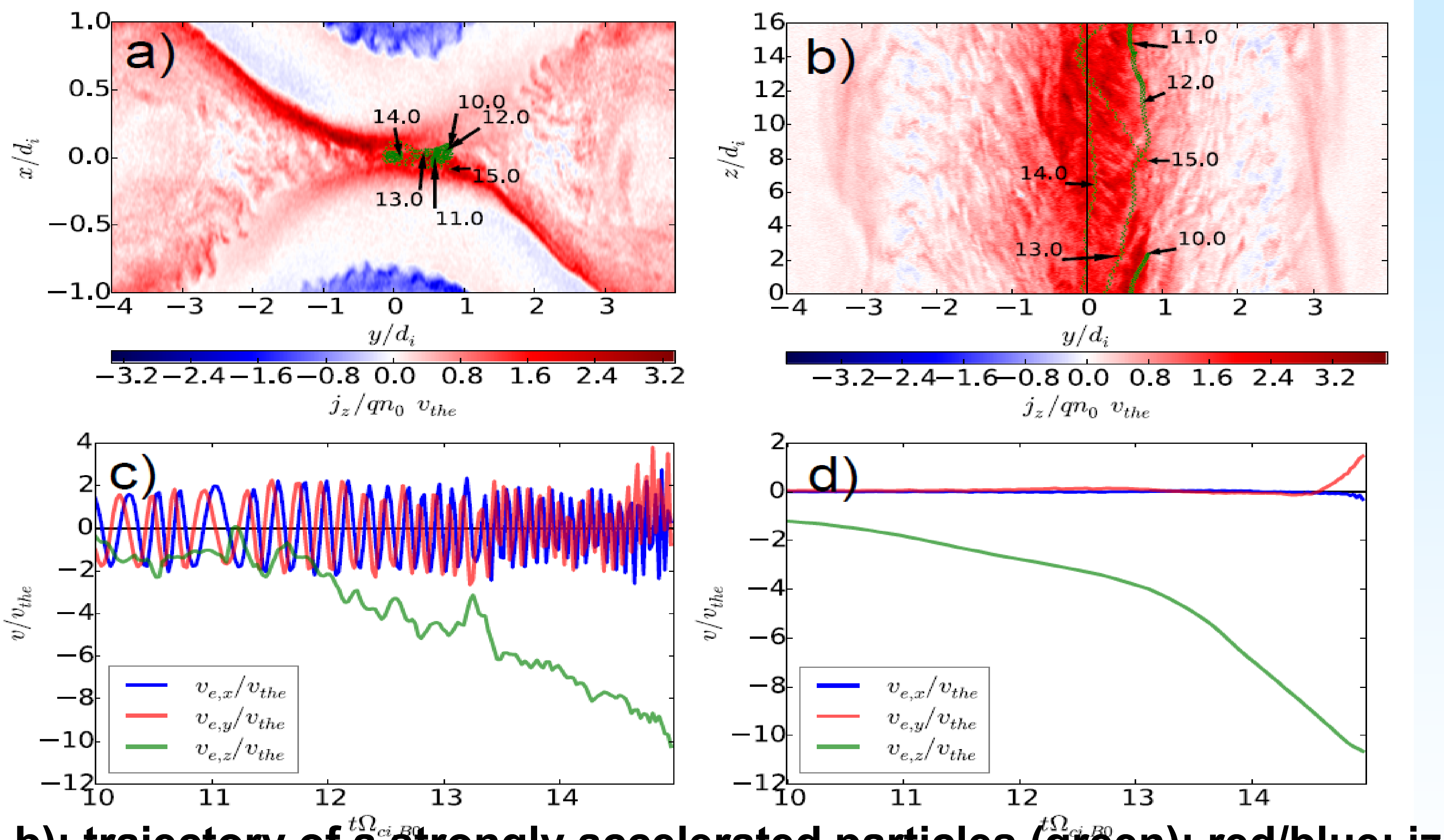

a) and b): trajectory of a strongly accelerated particles (green); red/blue: jz in the two planes at times of the nonlinear stage c) Velocity components of a typical strongly accelerated electron d) Temporary evolution of the average (four-) velocity components of the 10^4 most energized electrons.

Resulting e⁻-energy distributions

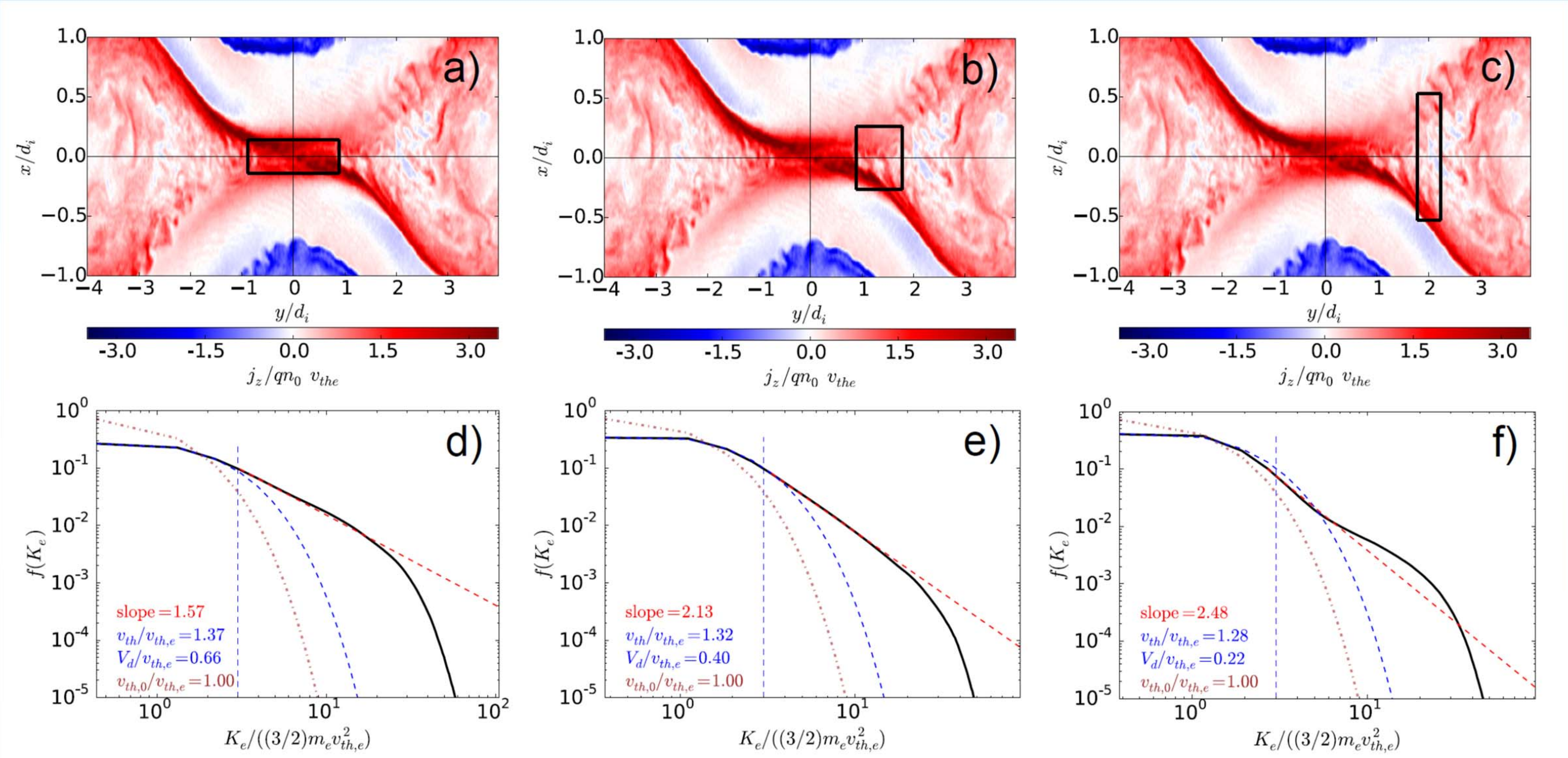

For t Ω_{ci} = 15 Top: (a)-(c) current density Jz in the plane x-y at z = center. Bottom: Distribution functions in the black boxes of the top-row-Figures: Lines: brown dashed-dotted: initial thermal distribution, blue dashed: Maxwellian fit to that distribution, red lines: power law fit to the energetic tail [Büchner et al,2018]

Resulting e⁻ -velocity distributions

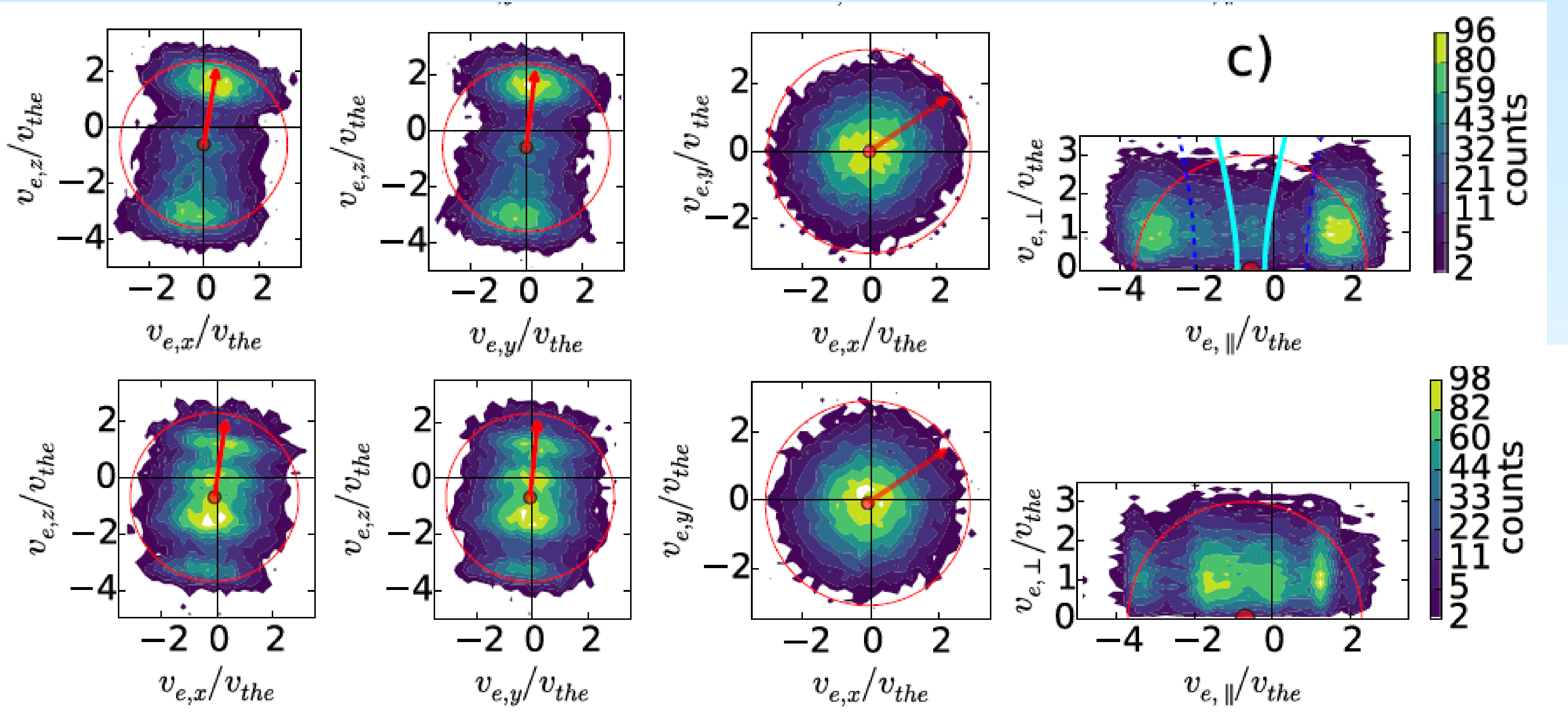

Resulting from of kinetic reconnection and the non-linear turbulence feed-back: energetic electron distributions become become counterstreaming ring-type beams

Incomplete ring-beam- (not horseshoe!) electron distributions

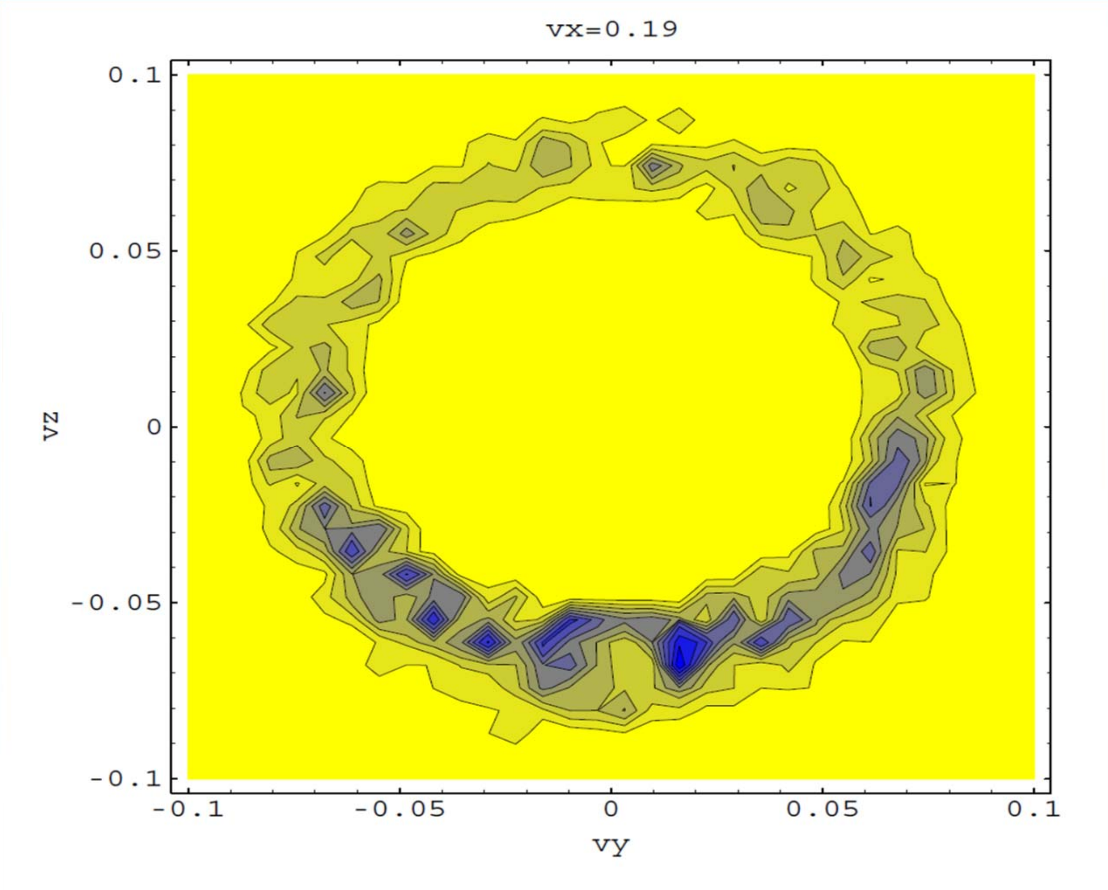

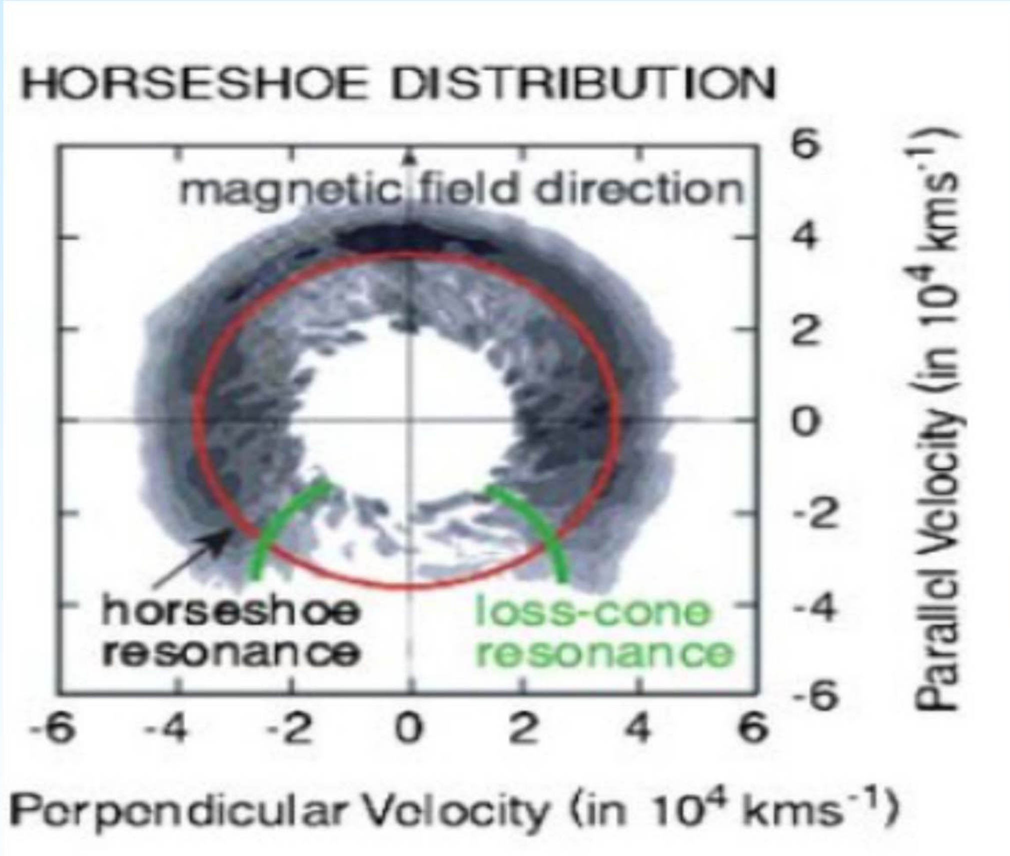

Incomplete ring distribution direction: perpendicular to B [from Büchner & Kuska, JGG].

Horseshoe distributions in magnetic mirrors are differently oriented!

Modeling radiative instabilities

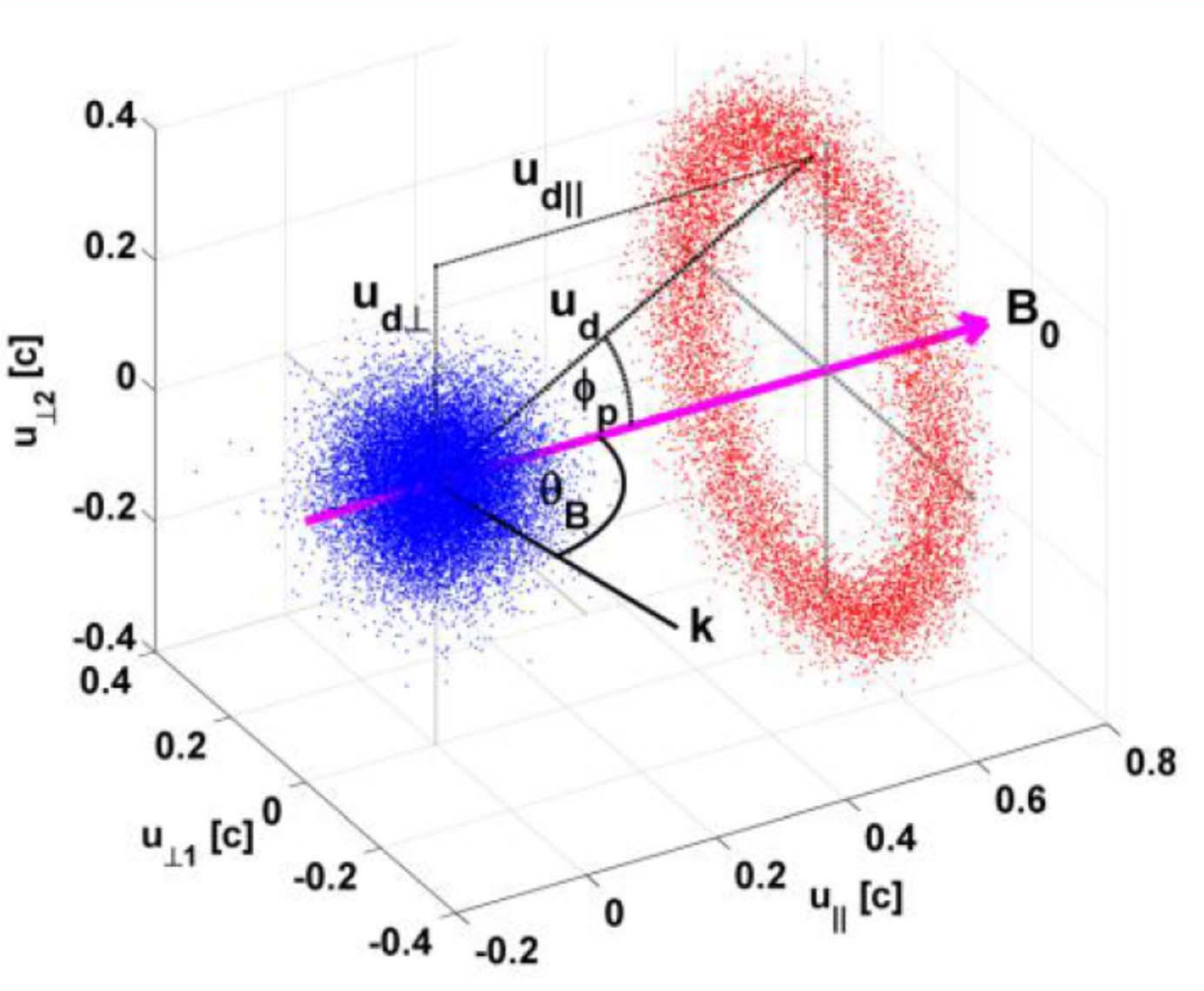

The radiation properties of reconnection-generated distributions remind that of bump-on-tail electron electron ring-distributions:

ECMI instability possible !

$$f_{rb}(u_{\|}, u_{\perp}) \propto n_{rb} exp\left[-\frac{(u_{\perp} - u_{d\perp})^2 + (u_{\|} - u_{d\|})^2}{2(\Delta u)^2}\right]$$

2.5 D PIC-code wave simulation

Initial electron distribution

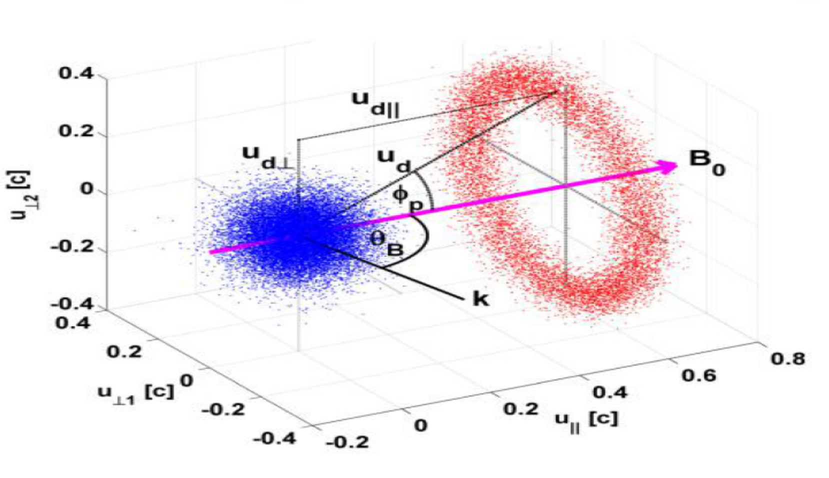

Numerical parameters

1024 x 1024 grid points;
M_p / m_e = 1836
periodic and open boundary conditions; 1000 particles / cell

$$\Delta t = (1/23.9)\omega_{pe}^{-1}$$

$$CFL : c\Delta t/\Delta x = 0.5.$$

Physical conditions / parameters

Uniform background magnetic field along X;

ω_{pe} = 5 x 10^9 rad/s;

Zero net-current, i.e.

$u_{background//} = - u_{ringbeam//} * n_{ringbeam} / n_{background}$

$\Delta u_{ringbeam}$ = 0.025c

$\Delta u_{background}$ = 0.05c

$\gamma=[1+(u_{rb\perp}{}^2 + u_{rb//}{}^2)/c^2]^{1/2}=1.2\sim 100keV$

$\tan(u_{ring\perp} / u_{ring//}) = 30^0$

n_{rb} / n_{total}= 0, 0.5 %, 1%, 2%, 3%, 4%, 5%

n_{total} fixed; Ω_{ce} / ω_{pe} = 5 … Ω_{ce}/ω_{pe} = 0.2

Intensity of unstable waves

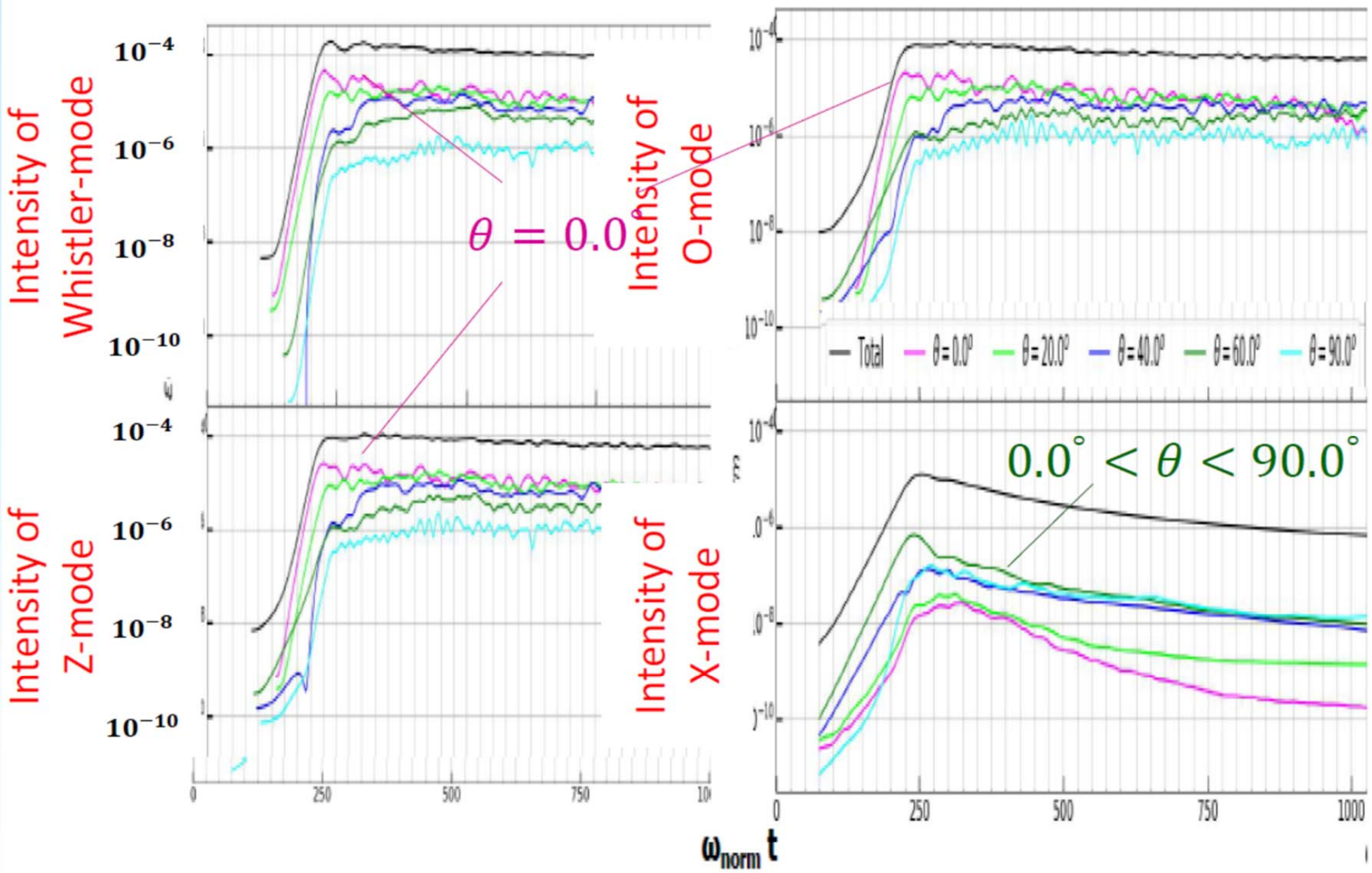

intensity of each mode increases and then saturates with time

energy:

$$\mathcal{E}_W > \mathcal{E}_Z > \mathcal{E}_O > \mathcal{E}_X$$

growth rate:

$$r_W, r_Z, r_O > r_X$$

Whistler, Z & O mode waves propagate mainly parallel to the B-field; obliquely escaping X-mode waves (ECM instability!) [Zhou, JB, 2019]

Ring-beam <-> pure beam-plasma instability: X-mode wave intensity

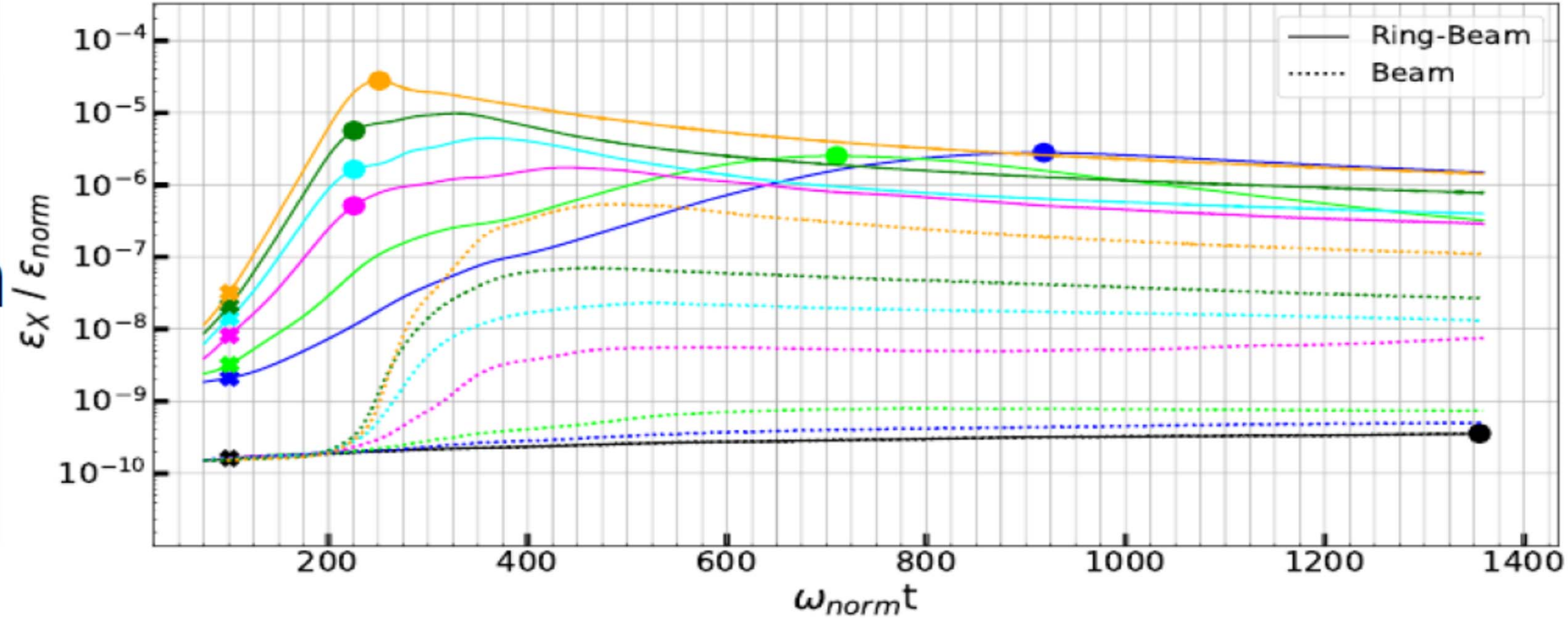

Intensity of escaping from density cavities ($\Omega_{ce} > \omega_{pe}$) X-mode waves in dependence on n_{beam}/n_{back} (colors). Ring+$V_{\|}$-gradient driven (ECMI, solid lines) vs. purely $V_{\|}$-gradient driven (bump-on-tail, dotted lines) waves [Zhou, Munoz, Büchner, 2019]

Reconnection diagnostis by solar type III radio burst observations

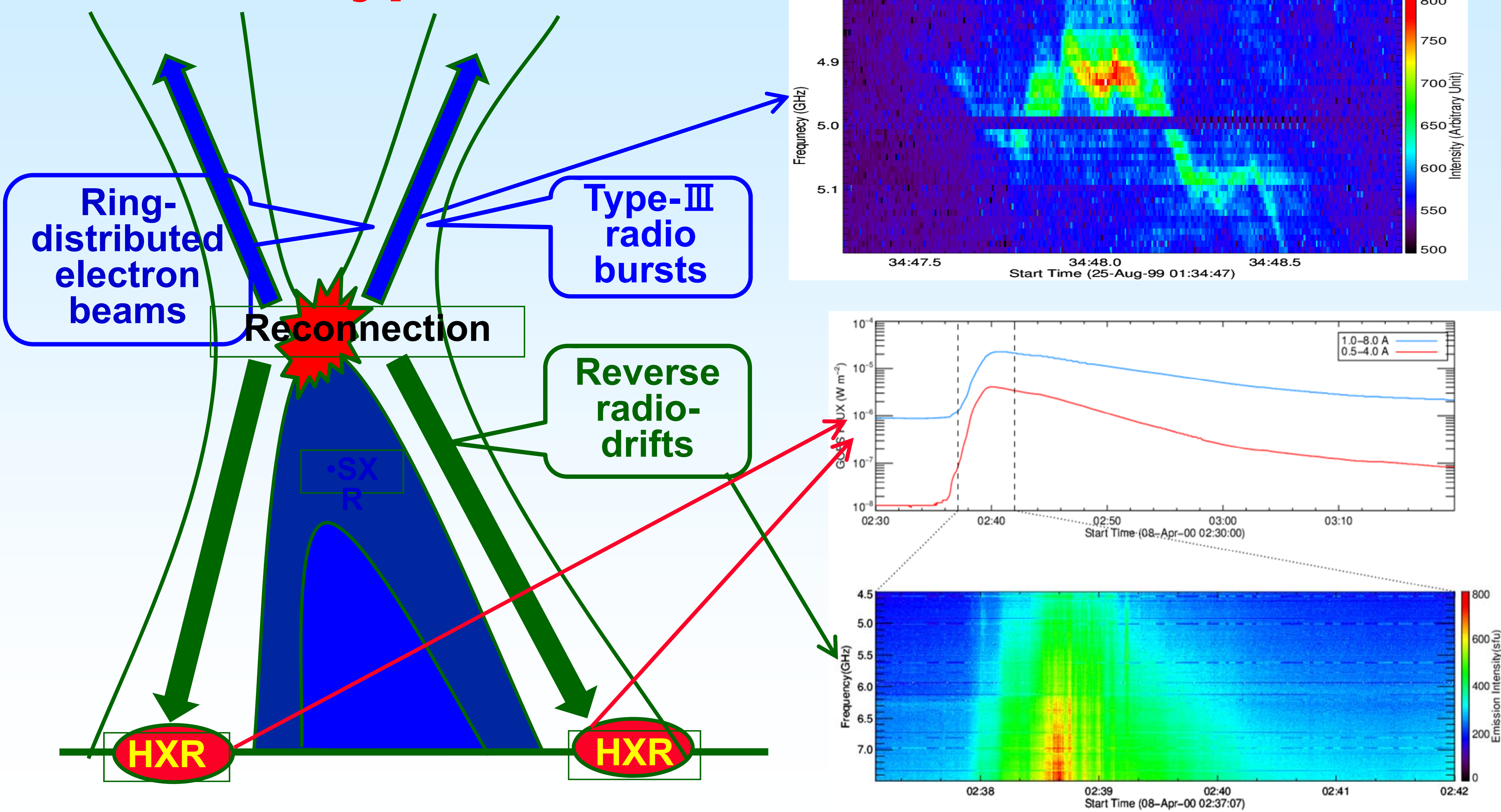

Summary

- In turbulent, high S / R_m, collsionless astro-plasmas strong guide-field reconnection can become very efficient, but not by „Efficient widenings of the (Parker-Sweet-) outflow region but by the creation of small scale current sheet / magnetic island strucures which cause efficient reconnection down to electron scales.
- Multiple reconnection in turbulence effectively heats the plasma and accelerates particles to high energies.
- The resulting distribution functions of accelerated electrons generate radio-signals which can be used for remote diagnostics of reconnection at the Sun and in other astroplasmas.

Resources used per simulation	3D	2D
# CPU cores	32768	4032
Memory [TB]	11	0.4
Total (aggregate) runtime [days]	5	6
Amount of data generated [TB]	0.7	0.1